

International Atomic Energy Agency

INDC(CCP)-7/U  
FEB 1970

---

**INDC**

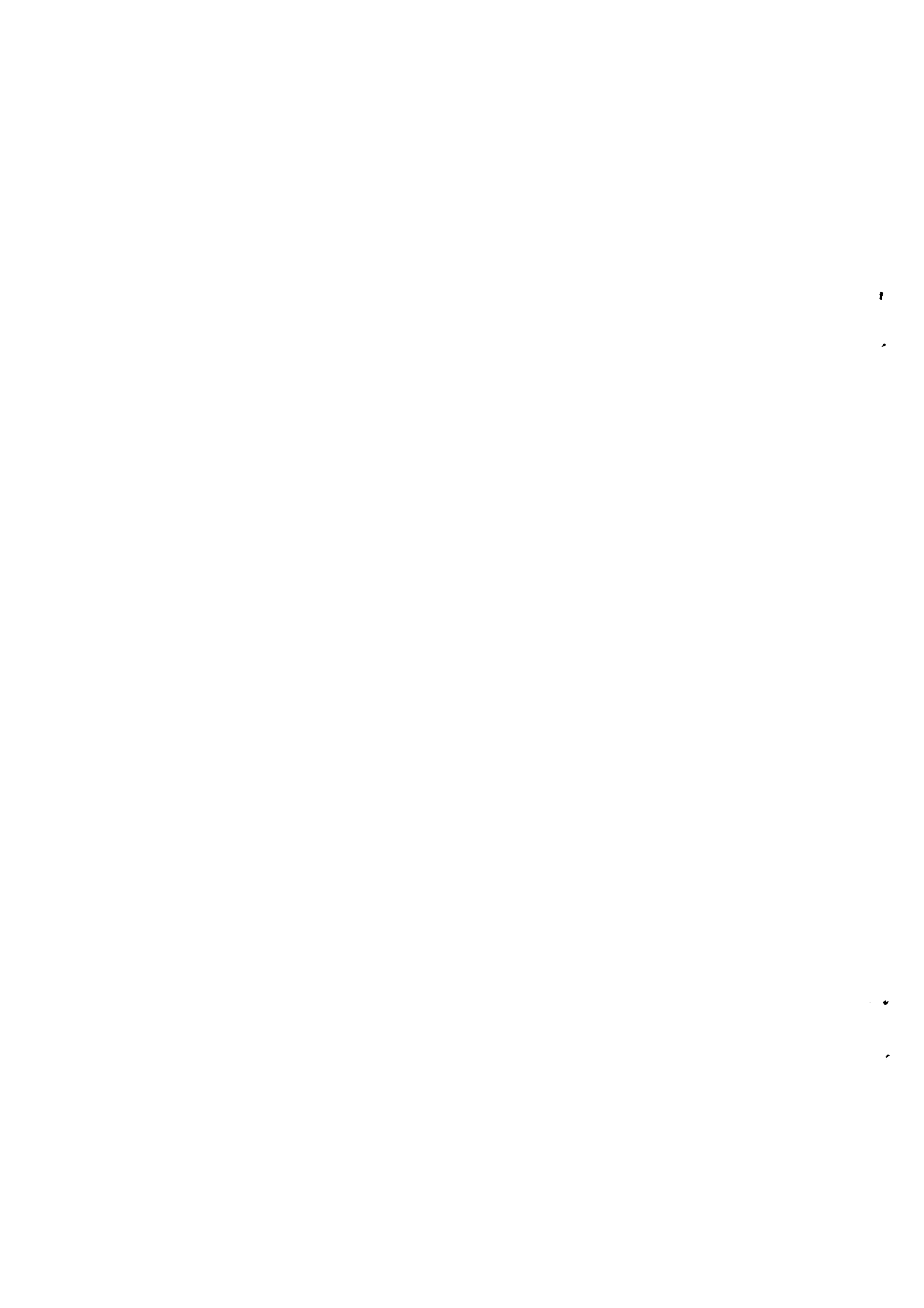
INTERNATIONAL NUCLEAR DATA COMMITTEE

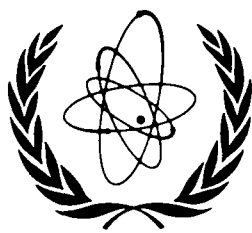
---

**USSR STATE COMMITTEE  
ON THE UTILIZATION OF ATOMIC ENERGY  
NUCLEAR DATA INFORMATION CENTRE**

**NUCLEAR PHYSICS RESEARCH IN THE USSR  
(Collected Abstracts)  
No. 7**

**English translation of an original in Russian  
published by Atomizdat, 1969**





International Atomic Energy Agency

INDC(CCP)-7/U  
FEB 1970

---

**INDC**

INTERNATIONAL NUCLEAR DATA COMMITTEE

---

**USSR STATE COMMITTEE  
ON THE UTILIZATION OF ATOMIC ENERGY  
NUCLEAR DATA INFORMATION CENTRE**

**NUCLEAR PHYSICS RESEARCH IN THE USSR  
(Collected Abstracts)**

**No. 7**

English Translation of:

**ЯДЕРНО-ФИЗИЧЕСКИЕ  
ИССЛЕДОВАНИЯ В СССР  
СБОРНИК АННОТАЦИЙ**

EDITORIAL BOARD

Yu.V. Adamchuk, V.N. Andreev, G.Z. Borukhovich, N.V. Ignatyuk,  
I.A. Korzh, V.A. Naumov, A.I. Obukhov, Yu.P. Popov,  
E.I. Shestoperova (Editor)

Russian original published by Atomizdat, 1969

Institute of Physics and Power Engineering<sup>\*/</sup>

ENERGY SPECTRA OF INELASTICALLY-SCATTERED  
NEUTRONS

O.A. Salnikov, G.N. Lovchikova,  
G.V. Kotelnikova, A.M. Trufanov  
and N.I. Fetisov

The authors present energy spectra of inelastically-scattered neutrons for an initial energy of 14.3 MeV. The spectra are obtained for different neutron scattering angles in the range  $30-150^\circ$  with an angular resolution of  $\pm 6^\circ$ .

The following elements are studied: uranium-238, thorium-232, niobium, copper, iron. The spectra are measured using the time-of-flight method with cylindrical geometry.

Spectra for the second neutron in the  $(n,2n)$  reaction are also given.

---

<sup>\*/</sup> Editor A.V. Ignatyuk.

ANGULAR DISTRIBUTIONS OF INELASTICALLY-SCATTERED NEUTRONS  
WITH AN INITIAL ENERGY OF 14.3 MeV

O.A. Salnikov, G.N. Lovchikova, A.A. Ivanov,  
G.V. Kotelnikova, V.I. Maroka, V.M. Matveev,  
A.M. Trufanov and N.I. Fetisov

Angular distribution measurements are given for inelastically-scattered neutrons with an initial energy of 14.3 MeV in respect of the following nuclei: Fe, Cu, Nb,  $^{238}\text{U}$ ,  $^{232}\text{Th}$ .

The measurements were made on a time-of-flight spectrometer with cylindrical geometry: spectrometer resolving time 5-7 nsec, path length 2 m, neutron recording threshold 100 keV.

The inelastically-scattered neutron spectra measured for different scattering angles ( $30-150^\circ$ ) were used to obtain relative differential inelastic-scattering cross-sections, nuclear temperatures, and nuclear level-density parameters.

CROSS-SECTIONS FOR THE FORMATION OF  $\gamma$ -QUANTA IN THE  $(n,n'\gamma)$   
REACTION ON FLUORINE, COBALT, ANTIMONY AND TANTALUM NUCLEI

D.L. Broder, A.F. Gamaly, A.I. Lashuk, B.V. Nesterov and  
I.P. Sadokhin

A Ge(Li) semiconductor detector was used to measure spectra of  $\gamma$ -quanta emitted in the inelastic scattering of neutrons on  $^{19}\text{F}$ ,  $^{59}\text{Co}$ , Sb and  $^{181}\text{Ta}$ .

Gamma quanta were observed with the following energies: for  $^{19}\text{F}$  -  $110 \pm 1$  and  $200 \pm 1$  keV; for  $^{59}\text{Co}$  -  $1095 \pm 2$ ,  $1190 \pm 2$ ,  $1280 \pm 2$  and  $1400 \pm 2$  keV; for Sb -  $153 \pm 1$  keV; for  $^{181}\text{Ta}$  -  $137 \pm 2$ ,  $153 \pm 2$ ,  $163 \pm 2$ ,  $302 \pm 2$ , and  $482 \pm 1$  keV.

Cross-sections for the formation of  $\gamma$ -quanta in the inelastic scattering process were determined for these energies. The results obtained are compared with the results of other authors and recommended cross-sections are given.

A PHENOMENOLOGICAL THEORY OF COLLECTIVE EXCITATIONS IN NUCLEI

N.S. Rabotnov and A.A. Seregin  
(Submitted to Jadernaja Fizika)

The authors discuss the dependence of the potential energy of nuclear deformation on the deformation parameters. It is shown that a potential of the form  $V = A + B\beta + C^2\beta + D\beta\cos 3\gamma$  is practically convenient. Given this form of potential, a numerical-solution method is proposed for the Schroedinger collective-model equation with five dynamic variables; the method does not assume that the fluctuations relative to the equilibrium deformation are small or that they are separate from rotation in adiabatic approximation. The positions of levels  $0+$ ,  $2+$ ,  $4+$  and  $6+$  are discussed and compared with experimental data for even-even nuclei.

SPIN DEPENDENCE OF THE DENSITY OF EXCITED NUCLEAR STATES

A.V. Ignatyuk, V.S. Stavinsky

The authors studied the effect of the discrete structure of a spectrum of single-particle nuclear states on the behaviour of the level-density spin dependence parameter  $\sigma^2$  and on the moment of inertia  $J_\mu$  relative to the axis of symmetry. The dependence of the mean-square projection of the nucleon moment  $\langle m^2 \rangle$  on mass number is calculated for single-particle levels of the Nilsson potential (Fig. 1). At sufficiently high nuclear-excitation energies the effect of the shell structure of  $\langle m^2 \rangle$  disappears, and the dependence of  $\langle m^2 \rangle$  on the mass number and the deformation parameter  $\beta$  is described by the solid-body relation:

$$\langle m^2 \rangle = (0.290 \pm 0.005) \times (1 - 2/3\beta) A^{2/3}.$$

The  $\langle m^2 \rangle$  dependence thus obtained is sufficiently close to the relation  $\langle m^2 \rangle \approx 0.24 A^{2/3}$  recently used in preparing experimental data on nuclear resonance density [1].

---

[1] ERBA, E., FACCHINII, U., SAETTA-MENICHELLA, E., *Energia Nucleare* 15 (1968) 54.

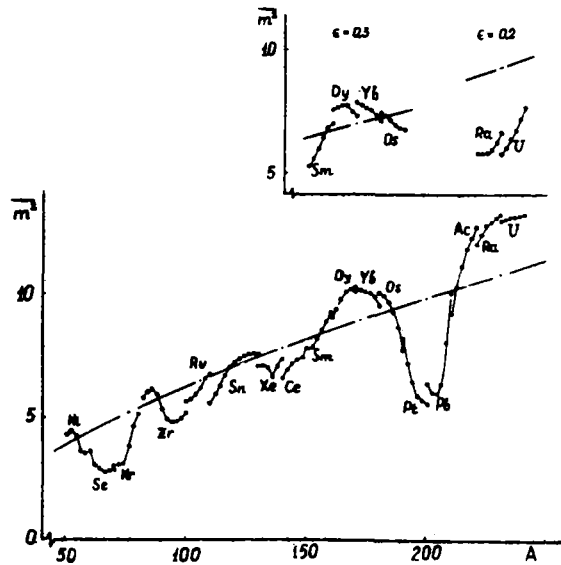


Fig. 1 Mean square of projection of angular momentum of nucleons on axis of symmetry  $\langle m^2 \rangle$ . Calculated from the non-interacting particle model for spherical nuclei and excitation energies of 7 MeV (—•—) and 100 MeV (—•—). Insert shows calculations for deformed nuclei.

LEVEL DENSITY OF NEAR-MAGIC NUCLEI

A.V. Ignatyuk, V.S. Stavinsky and Yu.N. Shubin

At present, experimental data on the thermodynamic characteristics of excited atomic nuclei are in most cases interpreted on the basis of analytical expressions obtained from the non-interacting particle model used in conjunction with a series of approximations [1]. Level-density calculations recently carried out [2] using a single-particle shell-model spectrum show that the energy dependence of the level density differs considerably from the Fermi gas case  $\rho \sim V^{-5/4} \exp [2 (aV)^{1/2}]$ . The paper includes a calculation of the thermodynamic characteristics of nuclei with a magic number of neutrons or protons.

It is shown that by taking into account the discrete structure of the single-particle spectrum it is possible to explain the constant "nuclear temperature" obtained from inelastically-scattered neutron spectra.

---

[1] ERICSON, T., Adv. Phys. 9 (1960) 425.

[2] IGNATYUK, A.V., SHUBIN, Yu.N., Jadernaja Fizika 8 (1968) 1135.

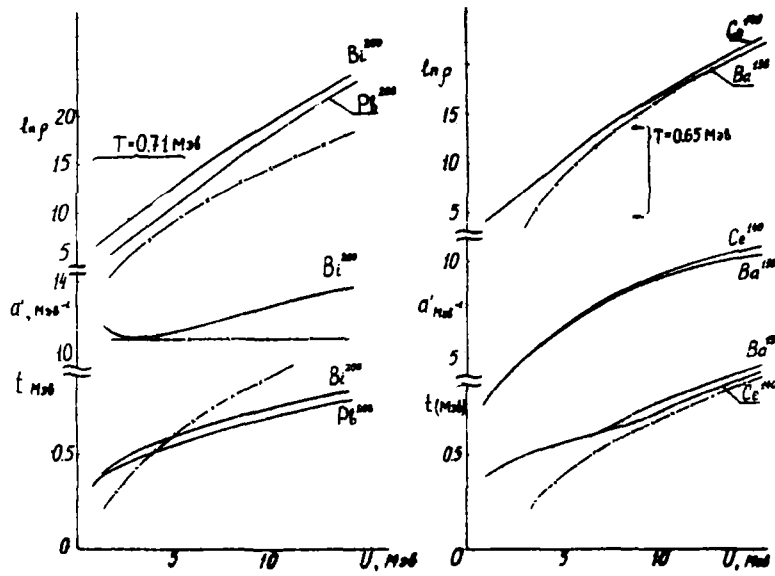


Fig. 1

Temperature, level density and parameter  $a'$  for  $^{138}\text{Ba}$ ,  $^{140}\text{Ce}$ ,  $^{208}\text{Pb}$  and  $^{209}\text{Bi}$  as functions of excitation energy. The small crosses indicate the Fermi-gas dependence of the respective quantities, allowance being made on a phenomenological basis for pairing [1].

EVEN-ODD DIFFERENCES AND FISSION BARRIER STRUCTURE

A.V. Ignatyuk, G.N. Smirenkin

The difference  $\Delta_f \approx 1.2$  MeV between the energy surfaces of odd and even nuclei, found from the systematics of observable fission barriers, is much greater than the analogous difference  $\Delta_0 = 0.7$  MeV for the ground states of heavy nuclei. Usually, the large magnitude of  $\Delta_f$  is attributed to increased pairing energy associated with nuclear deformation.

On this hypothesis, however, it is not possible to explain (a) the absence of barrier splitting with odd and odd-odd nuclei and the associated absence of "forbidden" spontaneous-fission periods for the odd-odd nuclei  $^{242}\text{Am}$  and  $^{254}\text{Es}$ , (b) the absence of splitting in the width ratio  $\Gamma_n/\Gamma_f$  for odd and odd-odd nuclei (Fig. 1).

These difficulties in interpreting the experimental data can be overcome with the hypothesis of the double-hump fission barrier [2]. In the double-hump barrier model the channel analysis results for the angular distributions of fragments in (d,pf) [3] and ( $\gamma$ ,f) [4] reactions must be referred to the second barrier B, whilst the neutron fission cross-section data must be referred to the higher, first barrier A. Thus, the difference in the barriers of even-even and odd nuclei found from the fission barrier systematics does not correspond to a higher pairing energy  $\Delta_f$ , but simply reflects a difference in the height of the barriers A and B. On the basis of this hypothesis all the experimental data on even-odd effects in nuclear fission can be interpreted for  $\Delta_f \approx \Delta_0 \approx 0.7$  MeV. For nuclei in the Th region barrier A is apparently no higher than barrier B so that here the experimental values of the fission thresholds show no difference in barrier height.

- 
- [1] HYDE, E.K., PERLMANN, I., SEABORG, G.T., Nucl. Prop. Heavy Elements, 1964 vol. I;  
SWIATECKI, W.J., Phys. Rev. 101 (1955) 97;  
VIOLA, V.E. Jr., WILKINS, B.D., Nucl. Phys. 82 (1966) 65.
- [2] STRUTINSKY, V.M., Nucl. Phys. A95 (1968) 420.  
STRUTINSKY, V.M., BJØRNHOLM, S., Int. Symp. Nucl. Structure, Dubna, 1968.
- [3] BRITT, H.C., RICKEY, F.A. Jr., HALL, A.W., LA-DC-9562 (1968).
- [4] RABOTNOV, N.S., et al., these abstracts.

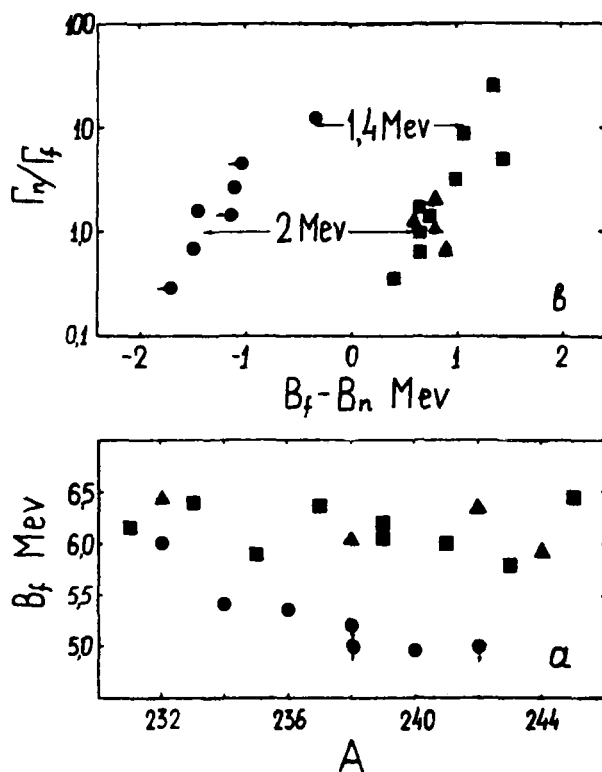


Fig. 1 (a) Fission threshold of even-even  $\bullet$ , odd  $\blacksquare$  and odd-odd  $\blacktriangle$  nuclei.  
 (b) Ratio of average neutron and fission widths as a function of the difference  $B_f - B_n$ , where  $B_f$  is the height of the fission barrier and  $B_n$  the neutron binding energy.

ANGULAR DISTRIBUTIONS OF FRAGMENTS IN  $^{238}\text{Pu}$  FISSION BY  
NEUTRONS OF ENERGY 0.06-7.20 MeV

D.L. Shpak, D.N. Stepanov, G.N. Smirenkin

(Submitted to *Jadernaja Fizika*)

"Tracking" methods (glass detectors) were used to measure the angular distributions of fragments for 10 angles and 5 neutron energies in the range  $E = 0.06-7.20$  MeV. The experimental data show the exceptional stability of the form  $W(\theta) = 1 + A \cos^2\theta$  right from the fission threshold and they are explained using the double-hump barrier concept [1]. The data for the energy dependence of angular anisotropy are extremely irregular and correspond to a step change in the parameter  $K^2$ . In the neighbourhood of the threshold of the  $(n, n'f)$  reaction there is a puzzling decrease in the angular anisotropy, practically down to zero.

REFERENCES

- [1] STRUTINSKY, V.M., BJØRNHOLM, S., Conf. Int. Simp. Nucl. Str.,  
Dubna, 1968.
- [2] VOROTNIKOV, P.E., et al., *Jadernaja Fizika* 3 (1966) 479.
- [3] VOROTNIKOV, P.E., et al., *Physics and Chemistry of Fission* 1,  
IAEA, Vienna (1965) 157.

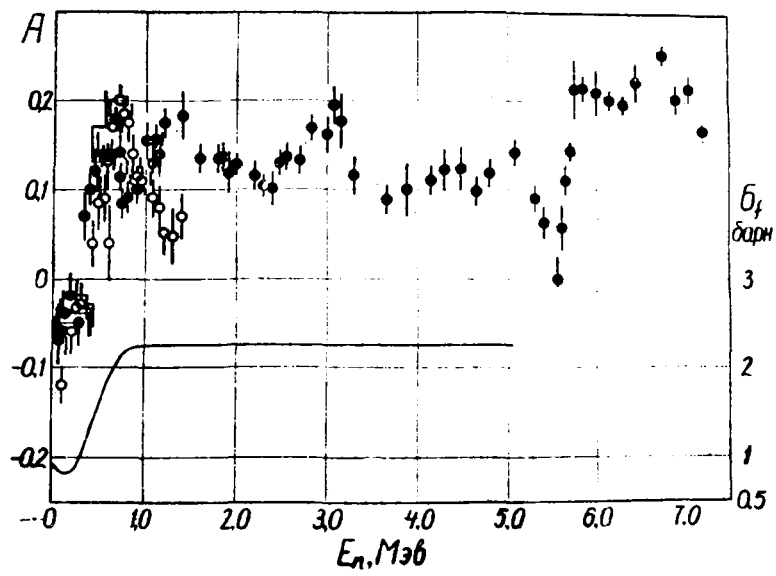


Fig. 1 Dependence of coefficient of angular anisotropy  $A$  on neutron energy  $E_n$  (o -  $\sqrt{2}$ ,  $\bullet$  -  $\sqrt{3}$ ,  $\bullet$  - this work).

ANGULAR ANISOTROPY OF  $^{241}\text{Am}$  NEUTRON-FISSION FRAGMENTS

D.L. Shpak, G.N. Smirenkin

(Submitted to Pisma ZWETF Journal of Experimental and Theoretical Physics Letters)

Tracking methods (cylindrical glasses) were used to measure the angular distributions of fragments  $W(\theta)$  in the fission of  $^{241}\text{Am}$  by neutrons in the energy range 0.3-7.2 MeV. The measured distributions agree satisfactorily with the relation  $W(\theta) = 1 + A \cos^2\theta$ . The values of the angular anisotropy coefficient  $A$  obtained in this work agree on the whole with the data given in reference [1] for the threshold energy region. The  $^{241}\text{Am}$  data together with analogous  $A$  data for other heavy nuclei are discussed in the light of the double-hump fission barrier concept.

REFERENCE

[1] VOROTNIKOV, P.E., et al., DAN 169 (1966) 314.

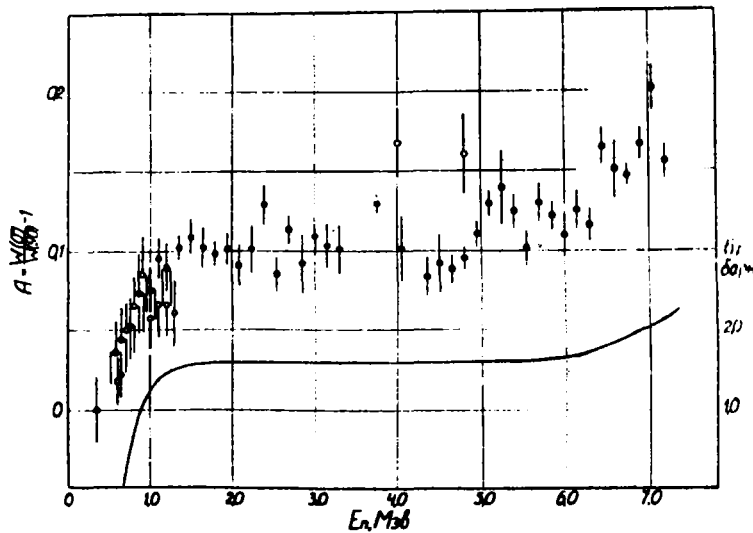


Fig. 1 Angular anisotropy of  $^{241}\text{Am}$  (n,f) fission fragments as a function of neutron energy (o - [1], ● - this study). The curve in the lower part is a schematic representation of the fission cross-section  $\sigma_f$ .

ANGULAR ANISOTROPY AND MASS ASYMMETRY OF FRAGMENTS IN  $^{235}\text{U}$   
AND  $^{238}\text{U}$  FISSION

V.G. Vorobeva, A.I. Gentosh, B.D. Kuzminov, A.I. Sergachev

(Submitted to Jadernaja Fizika)

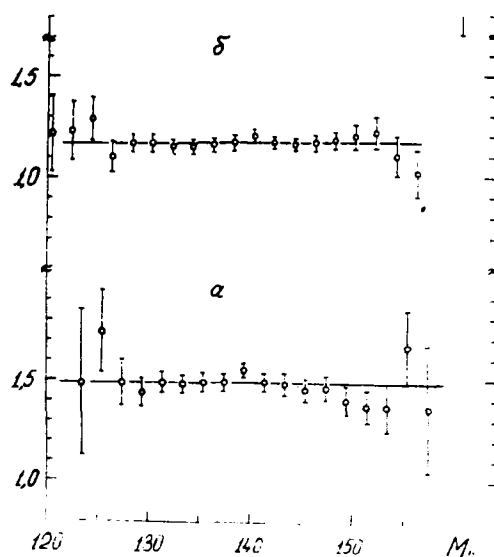
The authors present measurements of the angular anisotropy of fragments in relation to their mass for  $^{235}\text{U}$  and  $^{238}\text{U}$  fission by neutrons of energy 3 MeV and 1.6 MeV, respectively.

The angular anisotropy of fragments of different mass is exactly the same, within the limits of statistical experimental error. The main results are given in the tables.

$\nu^{235}$					
M	122,5	124,5	126,5	128,5	130,5
$\sigma(0^\circ)/\sigma(90^\circ)$	$1,23 \pm 0,14$	$1,29 \pm 0,11$	$1,1 \pm 0,08$	$1,17 \pm 0,05$	$1,17 \pm 0,04$
M	132,5	134,5	136,5	138,5	140,5
$\sigma(0^\circ)/\sigma(90^\circ)$	$1,15 \pm 0,04$	$1,15 \pm 0,04$	$1,16 \pm 0,03$	$1,17 \pm 0,03$	$1,20 \pm 0,03$
M	142,5	144,5	146,5	148,5	150,5
$\sigma(0^\circ)/\sigma(90^\circ)$	$1,17 \pm 0,03$	$1,16 \pm 0,03$	$1,17 \pm 0,04$	$1,18 \pm 0,04$	$1,20 \pm 0,06$
M	152,5	154,5	156,5		
$\sigma(0^\circ)/\sigma(90^\circ)$	$1,22 \pm 0,08$	$1,1 \pm 0,10$	$1,02 \pm 0,12$		
$\nu^{238}$					
M	123,5	125,5	127,5	129,5	131,5
$\sigma(0^\circ)/\sigma(90^\circ)$	1,49	1,74	1,49	1,44	1,49
M	133,5	135,5	137,5	139,5	141,5
$\sigma(0^\circ)/\sigma(90^\circ)$	1,48	1,49	1,49	1,55	1,49
M	143,5	145,5	147,5	149,5	151,5
$\sigma(0^\circ)/\sigma(90^\circ)$	1,48	1,45	1,46	1,40	1,37

$M$	153,5	155,5	157,5
$\sigma(0^\circ)/\sigma(90^\circ)$	1,37	1,66	1,46

$M$  Heavy fragment mass



GEOMETRICAL MODEL OF SYMMETRICAL FISSION. DYNAMICS: CALCULATION  
OF EFFECTIVE MASS

V.S. Stavinsky, N.S. Rabotnov, A.A. Seregin

(Submitted to Jadernaja Fizika)

The single-parameter geometrical model of symmetrical fission proposed in reference [1] is used, in conjunction with the liquid drop model, to calculate the dependence of the effective mass of a fissioning nucleus on the distance between the centres of gravity of fragments. In the progression through all the fission stages from the initial sphere to the two spherical fragments at infinity the effective mass changes from 0.533 to 0.25 of the total mass of the fissioning nucleus. Taking into account the changes in the effective mass in calculating the fission barrier penetrability there is an increase of about 10% in the logarithm of the life-time relative to spontaneous fission, but there is practically no effect on the energy dependence of the penetrability.

REFERENCE

- [1] STAVINSKY, V.S., RABOTNOV, N.S., SEREGIN, A.A., "Jadernaja Fizika" 7 (1968) 1051.

RADIATIVE CAPTURE OF FAST NEUTRONS BY THE  $^{238}\text{U}$  NUCLEUS  
IN THE ENERGY RANGE 0.01-15 MeV

V.A. Tolstikov

The paper contains an analysis of experimental measurements of averaged cross-sections for radiative capture of fast neutrons by the  $^{238}\text{U}$  nucleus. The relative measurements are renormalized to the presently accepted reference cross-sections. The results of the analysis are used to construct a recommended curve for the dependence of  $\sigma(n,\gamma)^{238}\text{U}$  on the neutron energy. The table shows the recommended values of  $^{238}\text{U}$  radiative capture cross-sections.

$E_n$ , keV	10	15	25	40	65	95
$\sigma(n,\gamma)$ , mb	614	570	460	368	260	206
$E_n$ , keV	145	210	285	385	525	835
$\sigma(n,\gamma)$ , mb	180	152	136	122	125	153

For  $E_n > 1$  MeV the recommended curve practically fits the data given by Barry [1] and Perkin [2], the accuracy of which also characterizes the accuracy of the values recommended in this energy range. For  $E_n < 1$  MeV, the accuracy of the  $\sigma(n,\gamma)$  curve is 3-4%.

The recommended curve for  $E_n < 1$  MeV comes below the curve of Vastel and Ravier [3].

On the basis of the perturbation theory [4], the authors estimate the effect of a change in the  $^{238}\text{U}$  group capture cross-sections on various fast assembly parameters.

- 
- [1] BARRY, J.F., BUNCL, J., WHITE, P.H., Journ. of Nucl. Energy 18 (1964) 481.  
 [2] PERKIN, J.Z., O'CONNOR, Z.R., COLEMAN, R.F., Proc. Phys. Soc. 72 (1958) 505.  
 [3] VASTEL, M., RAVIER, J., Proceedings of the Conference on Nucl. Cross-Sections and Technology, Washington, March 4-7, 1968, p. 1129.  
 [4] USACHEV, L.N., ZARITSKY, S.M., Nuclear Data for Reactors, Vienna 1967.

THE STATISTICS OF  $^{235}\text{U}$  FISSION WIDTHS BASED ON THE  
GENERALIZED PORTER-THOMAS DISTRIBUTION

A. Lukyanov and M.O. Shaker

A statistical distribution of  $^{235}\text{U}$  resonance fission widths is analysed on the basis of the generalized Porter-Thomas distribution, which depends on the number of channels for the fission process and on the relative contribution of these channels to the mean fission widths with a given total moment  $J$  (for  $^{235}\text{U}$  equal to  $3^-$  or  $4^-$ ). The "double-hump" which has been reported independently by several authors in the experimental histogram for the fission-width distribution, is connected with the facts that there is a considerable difference in the mean widths for  $J = 3^-$  and  $J = 4^-$  and that a relatively large number of fission channels is assumed for both states.

Under the terms of the hypothesis that compound-nucleus fission is possible after preliminary emission of a soft  $\gamma$  quantum (the so-called  $(n,\gamma,f)$  process), the number of channels for states with  $J = 4^-$  is assumed to be large, with an approximately equal probability of contributions from each channel. For states with  $J = 3^-$  both the  $(n,\gamma,f)$  process and direct fission are assumed: with the former process the number of channels is again assumed to be relatively large whilst the number of channels for the latter process is assumed to be small (approximately 1.2), which permits a qualitative explanation of the presence of a considerable number of resonances with large widths in the distribution (distribution tail).

On the basis of the analysis, the mean fission widths are estimated for each of the states -  $\bar{\Gamma}_{f4^-} = 25$  mV,  $\bar{\Gamma}_{f3^-} = 97$  mV; the first of these states corresponds to a number of channels  $\nu_4^- \approx 6$  and the second state represents the sum of two approximately equal widths, for the first of which the number of channels is equal to  $\nu_{3^-}^{(1)} \approx 12$  and for the second  $\nu_{3^-}^{(2)} \approx 2$ .

A MULTI-LEVEL SCHEME FOR THE ANALYSIS OF RESONANCE CROSS-SECTIONS

A.A. Lukyanov, A.V. Ignatyuk, V.P. Lunev

The problem of analysing the detailed structure of neutron cross-sections in the resonance range arises both from the greatly improved experimental resolution for energies at which there is considerable inter-resonance interference and from the need, which has developed in connection with recent reactor construction, for more accurate knowledge concerning the cross-section energy structure of a number of elements.

In the case of fissionable nuclei, the resonance structure cannot be represented as a superposition of single-level (Breit-Wigner) cross-sections, even for low-energy levels, particularly in the inter-resonance region. Interference between resonances causes resonance asymmetry and an anomalously low (or high) cross-section between resonances compared with the sum of two (or more) Breit-Wigner cross-sections. The need for a set of parameters to describe the cross-section structure in an interval containing several mutually interfering resonances leads to multi-level analysis schemes. For these purposes, the authors propose the use of cross-section parameters based on the Humbbet-Rosenfeld formalism [1]:

$$\sigma_n(E) = \pi \lambda^2 \sum_k \frac{\alpha_k \nu_k + \beta_k (M_k - E)}{(M_k - E)^2 + \nu_k^2}$$

where the parameters  $\alpha_k$ ,  $\beta_k$ ,  $M_k$  and  $\nu_k$  in the limited energy range  $\Delta E \ll E$  can be regarded as independent of energy.

To illustrate the method the authors analyse the fission cross-section for  $^{239}\text{Pu}$  (taking account of Doppler broadening and finite resolution) and work out a set of parameters for the energy range 20-55 eV to characterize all the important details of the resonance structure in the given range. With a two-level approximation (taking into account the interaction of only a pair of neighbouring levels with identical spin) the authors obtain resonance parameters  $\Gamma_{kn}$ ,  $\Gamma_{kf}$ ,  $\Gamma_k$  and the so-called "cross-widths"  $\Gamma_{kk'f}$  corresponding to the degree of inter-resonance interference.

---

[1] HUMBLET, J., ROSENFELD, L., Nucl. Phys. 26 (1961) 529.

THE TWO-HUMP BARRIER AND NEUTRON FISSION

E.V. Gai, A.V. Ignatyuk, N.S. Rabotnov, G.N. Smirenkin  
(Submitted to Jadernaja Fizika)

A quasi-classical approximation is used to calculate the energy dependence of the penetrability of a two-hump potential barrier with a well between the maxima. The detailed energy dependence of the penetrability is described by the formula:

$$P(E) = P_A P_B / 4 \{ [(P_A + P_B) / 4]^2 \sin^2 \phi(E) + \cos^2 \phi(E) \}^{-1}$$

where  $\phi(E) = \frac{1}{\hbar} \int_{\text{over the well}} P dx$  and  $P_A$  and  $P_B$  represent the penetrations of the two

maxima separately. This dependence has sharp maxima, coinciding with the positions of the quasi-levels in the well

$$P_{\max} = 4P_A P_B / (P_A + P_B)^2; \quad P_{\min} = P_A P_B / 4.$$

The energy-averaged penetration value  $\bar{P} = P_A P_B / (P_A + P_B)$ , which practically coincides with the penetrability of the higher "hump".

An expression is also derived for the statistical distribution of fission widths and compared with the experimental data for  $^{237}\text{Np}$  [1] in Fig. 1.

The authors discuss the possible experimental implications of the model discussed and compare them with nuclear data for neutron fission.

---

[1] FUBINI, A., BLONS, J., MICHAUDON, A., PAYA, D., Phys. Rev. Lit. 20  
(1968) 1373.

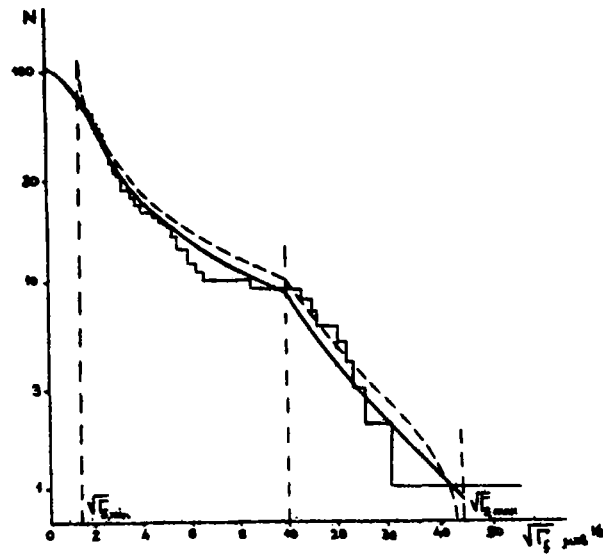


Fig. 1 Comparison between experimental and calculated fission-width distributions for  $^{237}\text{Np}(n,f)$  reaction. Histogram = experimental data from [1]; continuous curves = theoretical calculations for  $\Gamma_{fmin} = 2.3 \times 10^{-3}$  MeV,  $\Gamma_{fmax} = 2$  MeV,  $\bar{\Gamma}_f = 6.8 \times 10^{-2}$  MeV.

PHOTOFISSION OF EVEN-EVEN NUCLEI AND  
FISSION-BARRIER STRUCTURE

N.S. Rabotnov, G.N. Smirenkin,  
A.S. Soldatov, L.M. Usachev  
(Institute of Physics and Power Engineering)  
S.P. Kapitsa, Yu.M. Tsipenyuk  
(Institute for Physical Problems, USSR  
Academy of Sciences)

Experimental data are presented on cross-sections and angular distributions of photofission fragments for various nuclei; some of these data have already been published [1]. They are analysed in the context of the two-hump barrier hypothesis [2,3], which would appear to explain various experimental facts that are sharply at variance with the traditional concept.

The angular distributions are presented in the form

$$W(\theta) = a + b \sin^2 \theta + c \sin^2 2 \theta$$

The relative values of the coefficients are determined from the fission-barrier penetrability ratios for different combinations of moment  $J$ , parity  $\pi$  and projection of moment on nuclear axes of symmetry  $K$ :

$$b/a \approx P(1^-,0)/P(1^-,1); \quad c/b \approx \frac{\sigma_{\gamma abs}^{2^+}}{\sigma_{\gamma abs}^{1^-}} \cdot \frac{P(2^+,0)}{P(1^-,0)}$$

If, in accordance with the hypothesis of O,BOR [4], the fission thresholds satisfy the relations  $E_f(1^-,1) > E_f(1^-,0) > E_f(2^+,0)$ , the energy dependence of the angular distributions can be stated qualitatively as follows: the ratios  $b/a$  and  $c/b$  increase with decreasing excitation energy. This conforms to the picture observed. At high energies, both ratios tend to 0, but in the sub-barrier region  $b/a$  reaches values of about 100 ( $^{232}\text{Th}$ ,  $E_{\max} = 5.4$  MeV) while  $c/b \approx 3$  ( $^{240}\text{Pu}$ ,  $E_{\max} = 5.2$  MeV). Serious difficulties are encountered, however, in trying to give a quantitative explanation. The penetrability ratio for two barriers with peaks of different height and curvature, generally speaking, depends non-monotonically on energy and has a maximum value at an energy coinciding with the top of the lower barrier. The total photofission cross-section close to the threshold is

$\sigma_f \approx \sigma_{\text{yabs}}^{l^-} P(l^-,0)/P(l^-,0)+\alpha$  where it is less than the neutron binding energy  $\alpha = 2\pi F/\bar{D} \ll 1$  ( $\bar{D}$  is the spacing between levels of the compound nucleus).  $\sigma_f$  is approximately comparable to the cross-section for formation of a compound nucleus and, consequently, becomes a plateau at  $P(l^-,1) \ll P(l^-,0)\alpha \approx \alpha \ll 1$ , i.e. at an energy (observed threshold  $T_f$ ) which is somewhat lower than  $E_f(l^-,0)$ . This situation is depicted schematically in Fig. 1(a). Fig. 2(a) gives the experimental results; it shows the fragment yields corresponding to the different components in the angular distribution, as functions of the maximum bremsstrahlung spectrum energy. These curves were used to get the energy dependence of the partial components of the photofission cross-sections converted to monochromatic quanta. Fig. 2(b) shows the corresponding energy dependence of  $b/a$ ,  $c/b$  and  $\sigma_f$ . It seems paradoxical in the light of the simple considerations given above, that the energy at which the anisotropy - ratio  $b/a$  - reaches a maximum is almost 1 MeV lower with the plutonium isotopes than the observed threshold  $T_f$ , whereas one would expect it to be higher than  $T_f$ . Quantitatively, there is a big discrepancy: where  $b/a$  reaches its maximum value, the photofission cross-section should approximately coincide in value with its plateau value and with  $\sigma_{\text{yabs}}^{l^-}$ , but actually it is about 100 times less. As we will now show, this is just what should be expected in the two-hump barrier model with  $E_A > E_B$  (see Fig. 1(b)).

The solution of the one-dimensional quasi-classical problem of determining the penetrability of the two-hump barrier shows that the mean penetrability is as it would be if there were only one barrier A, i.e. the position of the observed threshold in the cross-section is determined by the higher barrier A. According to Strutinsky and Bornholm [3] the mechanism for the appearance of anisotropy is then as follows: having passed the first barrier, the nucleus spends sufficient time in the second well to "forget" the value of  $K$  with which it passed through the first barrier. When  $E_{fB}^{l^-,0} < E < E_{fA}^{l^-,0} < E_{fA}^{l^-,1}$ , therefore, the nuclei enter the second well through the channel  $l^-,0$  on barrier A, if the energy is suitable, and then they fission, and the angular distribution is determined by the position of the excitation energy  $E$  in relation to the channels of barrier B. In this case  $T_f$  (i.e. the fission threshold observed from the cross-section), coincides approximately with  $E_{fA}^{l^-,0}$  for barrier A (or is somewhat lower than this threshold), while the maxima of the ratios  $b/a$  and  $c/b$  correspond approximately to energies  $E_{fB}^{l^-,0}$  and  $E_{fB}^{2^+,0}$  for barrier B (see Fig. 2(b)). The experimental picture is in complete agreement with this description and, on analysis, yields the following threshold values:

	$E_{fB}^{2+,0}$	$E_{fB}^{1-,0}$	$T_{fA}^{1-,0} (\sim E_{fB}^{1-,0})$	$\Delta_{AB}$
$^{232}\text{Th}$	5.7	5.9	5.9	0
$^{238}\text{U}$	5.0	5.4	5.6	0.2
$^{238}\text{Pu}$	5.2	5.4	6.1	0.7
$^{240}\text{Pu}$	5.0	5.1	6.0	0.9
$^{242}\text{Pu}$	5.0	5.2	6.1	0.9

$\Delta_{AB} = T_f - E_{fB}^{1-,0}$  increases from thorium to plutonium in the manner explained in reference [3]. Since in most cases c/b increases monotonically with decreasing energy for  $E_{fB}^{2+,0}$  as determined from the position of the maximum of this ratio, the table gives the upper values.

- 
- [1] RABOTNOV, N.S., SMIRENKIN, G.N., SOLDATOV, A.S., USACHEV, L.N., KAPITSA, S.P., TSIPENYUK, Yu.M., Phys. and Chem. of Fission, Vol. 1, IAEA, Vienna, (1965) 135; Phys. Let. 268 (1968) 218.
- [2] STRUTINSKY, V.M., Nucl. Phys. A95 (1967) 420.
- [3] STRUTINSKY, V.M., BJØRNHOLM, S., Paper presented at the international symposium on nuclear structure, Dubna, 1968.
- [4] BOR, O., International Conference on the Peaceful Uses of Atomic Energy, Geneva, 1955, Fizmatgiz, p. 175 (1958).

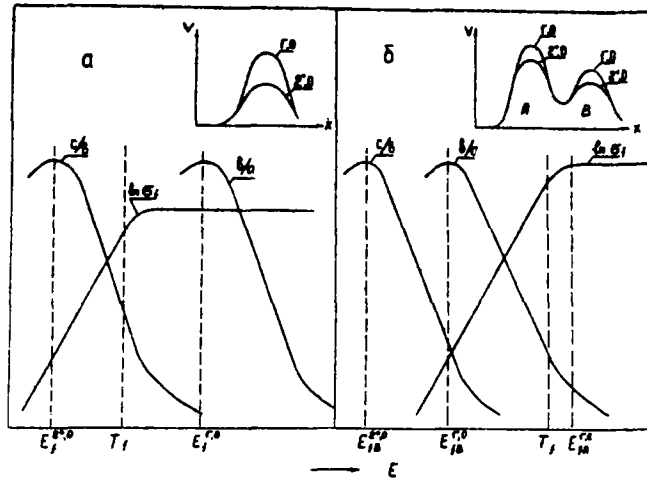


Fig. 1. Schematic representation of the energy dependence of anisotropy and fission cross-section for single-hump (a) and double-hump (b) barriers.

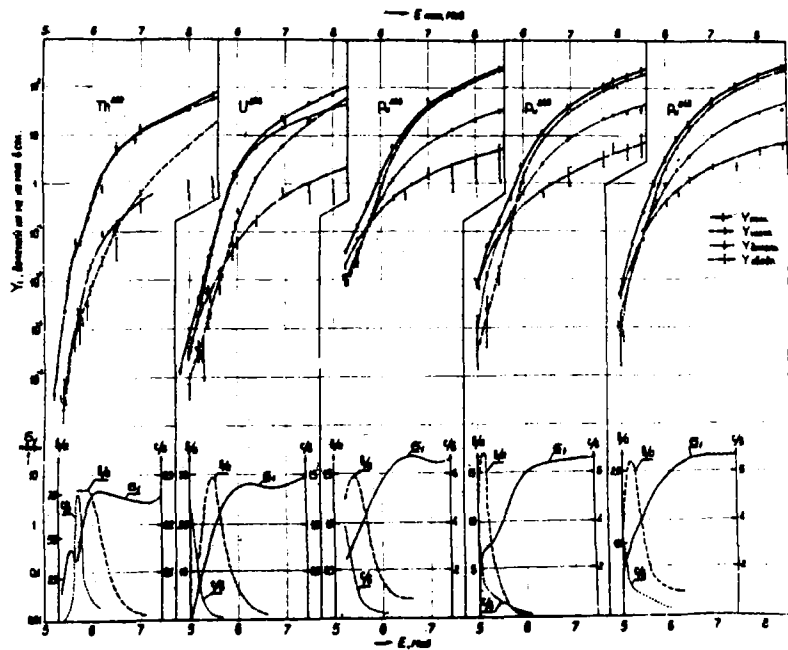


Fig. 2a Fragment yield measurements corresponding to different components of angular distribution and their dependence on the limiting energy of the bremsstrahlung spectrum.

Fig. 2b Fission cross-section and ratios  $b/a$  and  $c/b$  as functions of  $\gamma$ -quanta energy; obtained by processing experimental data.

I.V. Kurchatov Atomic Energy Institute<sup>\*/</sup>

CROSS-SECTIONS AND ANGULAR DISTRIBUTIONS OF FRAGMENTS IN THE FISSION OF  
<sup>238</sup>Pu, <sup>242</sup>Pu AND <sup>241</sup>Am BY NEUTRONS OF ENERGY 0.45-3.6 MeV

V.F. Fomushkim, E.K. Gutnikova  
(submitted to *Jadernaja Frizaka*)

The fission cross-section ratios of <sup>238</sup>Pu, <sup>242</sup>Pu, <sup>241</sup>Am and <sup>235</sup>U were measured using dielectric detectors on an electrostatic accelerator; the angular distributions of fragments of these isotopes were also measured. The measurements were made at 14 neutron energies in the range 0.45-3.6 MeV. Fission fragments were recorded at five angles  $\theta = 0^\circ, 22.5^\circ, 45^\circ, 67.5^\circ$  and  $90^\circ$  to the neutron beam. The results are given in Tables I and II. ( $a_0, a_2, a_4$  are the coefficients for the corresponding Legendre polynomials, with the sum of which the angular distributions of the fragments were approximated).

---

<sup>\*/</sup> Editor Yu.V. Adamchuk.

Table II

Isotope $E_n$ (MeV)	$Pu^{238}$		$Pu^{242}$		$Am^{241}$	
	$a_2/a_0$	$a_4/a_0$	$a_2/a_0$	$a_4/a_0$	$a_2/a_0$	$a_4/a_0$
$3.62 \pm 0.09$	$0.070 \pm 0.018$	$-0.031 \pm 0.025$	$0.115 \pm 0.026$		$-0.003 \pm 0.015$	
$3.34 \pm 0.08$	$0.092 \pm 0.015$		$0.124 \pm 0.036$	$-0.083 \pm 0.043$	$-0.025 \pm 0.016$	
$3.06 \pm 0.08$	$0.091 \pm 0.025$	$-0.056 \pm 0.036$	$0.189 \pm 0.028$		$0.037 \pm 0.019$	$-0.024 \pm 0.024$
$2.79 \pm 0.07$	$0.056 \pm 0.016$		$0.084 \pm 0.027$		$0.057 \pm 0.015$	
$2.51 \pm 0.07$	$0.081 \pm 0.019$		$0.121 \pm 0.039$	$-0.057 \pm 0.047$	$0.012 \pm 0.015$	
$2.23 \pm 0.06$	$0.077 \pm 0.017$	$-0.027 \pm 0.021$	$0.116 \pm 0.020$		$0.015 \pm 0.018$	$0.036 \pm 0.022$
$1.96 \pm 0.06$	$0.090 \pm 0.011$		$0.166 \pm 0.018$		$0.047 \pm 0.015$	$-0.022 \pm 0.017$
$1.68 \pm 0.05$	$0.092 \pm 0.016$	$0.038 \pm 0.020$	$0.122 \pm 0.019$		$0.036 \pm 0.010$	
$1.40 \pm 0.05$	$0.076 \pm 0.011$		$0.169 \pm 0.019$		$0.040 \pm 0.012$	
$1.21 \pm 0.05$	$0.084 \pm 0.016$	$-0.093 \pm 0.019$	$0.249 \pm 0.025$	$-0.096 \pm 0.031$	$0.024 \pm 0.017$	$-0.034 \pm 0.020$
$1.02 \pm 0.05$	$0.077 \pm 0.026$	$-0.068 \pm 0.032$	$0.198 \pm 0.031$		$-0.014 \pm 0.030$	$0.074 \pm 0.036$
$0.83 \pm 0.05$	$0.111 \pm 0.027$		$0.272 \pm 0.050$		$0.019 \pm 0.061$	$-0.040 \pm 0.070$
$0.64 \pm 0.05$	$0.109 \pm 0.028$		$-0.082 \pm 0.073$	$0.500 \pm 0.087$	$-0.070 \pm 0.074$	$0.046 \pm 0.092$
$0.44 \pm 0.05$	$0.050 \pm 0.023$		$0.230 \pm 0.094$		$0.193 \pm 0.115$	

Table I

Isotope $E_n$ (MeV)	$Pu^{238}$		$Pu^{242}$		$Am^{241}$	
	$\sigma_{Pu^{238}} / \sigma_{Pu^{235}}$	$\sigma_{Pu^{238}}$	$\sigma_{Pu^{242}} / \sigma_{Pu^{235}}$	$\sigma_{Pu^{242}}$	$\sigma_{Am^{241}} / \sigma_{Pu^{235}}$	$\sigma_{Am^{241}}$
3,62 ± 0,09	2,03 ± 0,11	2,30 ± 0,13	1,04 ± 0,06	1,18 ± 0,07	1,77 ± 0,08	2,00 ± 0,09
3,34 ± 0,08	1,94 ± 0,10	2,23 ± 0,12	1,15 ± 0,06	1,32 ± 0,07	1,58 ± 0,06	1,82 ± 0,07
3,06 ± 0,08	1,90 ± 0,09	2,24 ± 0,11	0,91 ± 0,05	1,07 ± 0,06	1,71 ± 0,06	2,02 ± 0,07
2,79 ± 0,07	1,78 ± 0,08	2,13 ± 0,10	0,93 ± 0,05	1,11 ± 0,06	1,54 ± 0,06	1,85 ± 0,07
2,51 ± 0,07	1,90 ± 0,08	2,37 ± 0,10	1,03 ± 0,05	1,29 ± 0,06	1,64 ± 0,06	2,05 ± 0,07
2,23 ± 0,06	1,76 ± 0,08	2,30 ± 0,10	1,03 ± 0,05	1,35 ± 0,06	1,41 ± 0,05	1,85 ± 0,06
1,96 ± 0,06	1,63 ± 0,07	2,12 ± 0,09	0,92 ± 0,05	1,20 ± 0,06	1,44 ± 0,05	1,87 ± 0,06
1,68 ± 0,05	1,74 ± 0,07	2,17 ± 0,09	0,96 ± 0,05	1,20 ± 0,06	1,38 ± 0,05	1,73 ± 0,06
1,40 ± 0,05	1,76 ± 0,07	2,15 ± 0,09	1,06 ± 0,05	1,29 ± 0,06	1,31 ± 0,05	1,60 ± 0,06
1,21 ± 0,05	1,70 ± 0,07	2,08 ± 0,09	1,19 ± 0,05	1,45 ± 0,06	1,22 ± 0,04	1,49 ± 0,05
1,02 ± 0,05	1,65 ± 0,07	2,01 ± 0,09	0,97 ± 0,06	1,18 ± 0,07	1,04 ± 0,04	1,27 ± 0,05
0,83 ± 0,05	1,63 ± 0,07	1,92 ± 0,08	0,71 ± 0,06	0,84 ± 0,07	0,57 ± 0,03	0,67 ± 0,04
0,64 ± 0,05	1,50 ± 0,07	1,70 ± 0,08	0,30 ± 0,03	0,34 ± 0,03	0,20 ± 0,02	0,23 ± 0,02
0,44 ± 0,05	0,96 ± 0,05	1,15 ± 0,06	0,08 ± 0,02	0,10 ± 0,03	0,055 ± 0,01	0,065 ± 0,01

Institute of Theoretical and Experimental Physics<sup>\*/</sup>

EXCITATION OF ANALOGUE STATES IN  $^{58,60}\text{Ni}$  (d,n)  $^{59,61}\text{Cu}$  REACTIONS

V.V. Okorokov, D.A. Tolchenkov and Yu.M. Cheblukov

Neutron spectra were measured for  $^{58,60}\text{Ni}$  (d,n)  $^{59,61}\text{Cu}$  reactions using the time-of-flight method on the Institute's cyclotron with deuteron energies  $E_d = 11.2 \pm 0.7$  MeV. The time analyser with a channel width of about 1 nsec works on the "nonius" principle.

The position of the resolved levels was determined for the finite  $^{59,61}\text{Cu}$  nuclei and the quantum ( $1_p$ ) and spectroscopic  $(2j + 1)c^2S$  characteristics were determined using the distorted wave method of analysis.

The maximum differential cross-section for the  $^{59,61}\text{Cu}$  levels, which are regarded as analogue states, were as follows:

$^{59}\text{Cu}$  ( $1_p = 1$ )  $E^* = 3.88$  (7.2; 4.33 (2.4); 4.79 (0.6); 5.19 (1.7), where the figures in brackets represent the cross-section in mbarn/ster and  $E$  is in MeV

$^{61}\text{Cu}$  ( $1_p = 1$ )  $E^* = 6.42$  (3.3); 6.68 (2.6);

( $1 = ?$ )  $E^* = 7.13$ ; 7.37; 7.62.

A comparison of the characteristics of these levels with those of low-lying levels excited in  $^{58,60}\text{Ni}$  (d,p)  $^{59,61}\text{Cu}$  reactions shows that the agreement between them is satisfactory.

---

<sup>\*/</sup> Editor V.N. Andreev.

A.F. Ioffe Physico-Technical Institute\*/  
USSR Academy of Sciences, Leningrad

FRAGMENT MASS AND ENERGY DISTRIBUTIONS IN NUCLEAR  
PHOTOFISSION OF  $^{232}_{92}\text{U}$ ,  $^{209}_{83}\text{Bi}$  AND  $^{197}_{79}\text{Au}$

A.P. Komar, B.A. Bogachov, A.A. Kotov, Yu.N. Ranyuk,  
G.G. Semenchuk, G.E. Solyakin, P.V. Sorokin

Semiconductor detectors were used on the Kharkov U-2000 linear accelerator to study the mass and energy distributions  $P(\mu, E_K)$  of pair fragments from nuclear photofission of  $^{232}_{92}\text{U}$  for  $E_{\gamma, \text{max}} = 250$  MeV,  $M, 600$  MeV and  $1000$  MeV and of  $^{209}_{83}\text{Bi}$  and  $^{197}_{79}\text{Au}$  at  $E_{\gamma, \text{max}} = 1000$  MeV. The experimental data show that in the nuclear fission of  $^{232}_{92}\text{U}$  the mass distribution remains asymmetrical up to  $E_{\gamma, \text{max}} = 1000$  MeV. The "dip" in the total kinetic energies of symmetrical fragments also remains.

The photofission of  $^{209}_{83}\text{Bi}$  and  $^{197}_{79}\text{Au}$  leads to a predominantly symmetrical mass distribution and a monotonic dependence of the total kinetic energy on the degree of mass asymmetry of the fragments. Data for the fission of  $^{209}_{83}\text{Bi}$  and  $^{197}_{79}\text{Au}$  are compared with predictions from the Niks-Svyatetsky theory. The main experimental results are given in the table.

Target nucleus	$E_K$ (experiment) MeV	$E_K$ corrected for neutron emission MeV	$\mu_{2E}$ (experiment) MeV	$\mu_{2M}$ (experiment) (atomic units) <sup>2</sup>
$^{232}_{92}\text{U}$	$168 \pm 3$	$171 \pm 3$	$163 \pm 4$	-
$^{209}_{83}\text{Bi}$	$138 \pm 3$	$146 \pm 3$	$171 \pm 4$	$272 \pm 5$
$^{197}_{79}\text{Au}$	$114 \pm 5$	$122 \pm 5$	$161 \pm 7$	$311 \pm 10$

\*/ Editor G.Z. Borukhovich.

ISOMERIC  $\gamma$ -RADIATION FROM NUCLEAR FRAGMENTS WITH  
EXCESS NEUTRONS IN THERMAL FISSION OF URANIUM-235

L.A. Popeko, G.V. Petrov, D.M. Kaminker

The authors studied the delayed  $\gamma$ -radiation of fragments from the thermal fission of uranium-235 in the time range 10-100 nsec after separation. A Ce(Li) detector with an energy resolution of 5.5 keV was used to analyse the gamma spectra. The  $\gamma$ -ray distribution as a function of fragment mass was analysed using a two-dimensional analyser. The experimental resolution was 8.5 mass units. The  $\gamma$ -ray distribution as a function of delay time was studied using a time-amplitude converter and a two-dimensional analyser. The time resolution of the Ce(Li) detector/surface barrier detector system was 18 nsec. The data are analysed in the table.

Evaluation of the isomeric-ratio yields for a number of nuclear fragments lends support to the hypothesis that the fragments acquire large angular moments in the separation process.

Table I

Light group				Heavy group			
M a.m.u	E keV	T I/2 nsec	I0 <sup>2</sup> quanta/fiss.	M a.m.u	E keV	T I/2 nsec	I0 <sup>2</sup> quanta/fiss.
91 ± 2	317 ± 2	10 ± 2	0,40 ± 0,1	132 ± 2	168 ± 1	12 ± 3	0,4 ± 0,2
92 ± 2	108 ± 1	40 ± 8	1,6 ± 0,3	133 ± 2	302 ± 1	10 ± 2	2,3 ± 0,4
	168 ± 1	12 ± 3	0,5 ± 0,2	134 ± 2	128 ± 1	40 ± 8	0,5 ± 0,2
	191 ± 1	12 ± 3	0,8 ± 0,3		160 ± 1	10 ± 2	0,3 ± 0,1
	278 ± 2	8 ± 2	1,1 ± 0,3	136 ± 2	143 ± 1	15 ± 3	0,5 ± 0,1
993 ± 2	123 ± 1	40 ± 8	0,7 ± 0,3		190 ± 1	10 ± 2	0,5 ± 0,2
	143 ± 1	16 ± 4	3,8 ± 0,6	138 ± 2	208 ± 1	15 ± 3	1,1 ± 0,3
94 ± 2	206 ± 1	15 ± 4	4,7 ± 0,8	139 ± 2	119 ± 1	40 ± 8	1,2 ± 0,2
	353 ± 2	11 ± 2	3,5 ± 0,6	140 ± 2	290 ± 2	8 ± 2	0,6 ± 0,3
99 ± 2	116 ± 1	40 ± 8	0,3 ± 0,2	141 ± 2	150 ± 1	10 ± 2	0,5 ± 0,1
102 ± 2	125 ± 1	40 ± 8	0,6 ± 0,2	143 ± 2	166 ± 1	10 ± 2	0,6 ± 0,2
	228 ± 2	8 ± 2	0,8 ± 0,3		108 ± 1	40 ± 8	0,3 ± 0,1
	158 ± 1	12 ± 3	0,5 ± 0,2		98 ± 1	40 ± 8	0,5 ± 0,2
	265 ± 2	8 ± 2	0,3 ± 0,2	145 ± 2	268 ± 2	8 ± 2	0,4 ± 0,2
104 ± 2	130 ± 1	40 ± 8	0,1 ± 0,1	148 ± 2	138 ± 1		
	185 ± 1	8 ± 2	0,5 ± 0,2		1300 ± 2	12 ± 4	2,0 ± 0,7
	168 ± 1	8 ± 2	0,4 ± 0,2				
	750 ±	12 ± 4	3,0 ± 0,7				

SOME CHARACTERISTICS OF  $\gamma$ -RADIATION ACCOMPANYING  
SPONTANEOUS FISSION OF  $^{252}\text{Cf}$

B.M. Alexandrov, I.A. Baranov,  
G.V. Valsky, A.S. Krivokhatsky,  
G.A. Petrov and Yu.S. Pleva

The  $\gamma$ -ray yield for energies greater than 100 keV was measured at angles of 30 and 90° to the axis of separation of fragments from the spontaneous fission of  $^{252}\text{Cf}$  as a function of the total kinetic energy of the fragments. The measurements were made by a method similar to one already described [1].

The data obtained were corrected for energy lost by the fragments and for the finite solid angle. In making the calculations it was assumed that the angular distribution of the radiation is of the form  $J(\theta) = J(90^\circ)(1 + A \cos^2\theta)$ . Energy calibration was carried out by comparison with the data given in reference [2]. The results obtained are given in the table. The mean square statistical errors are shown in columns 4 and 6.

[1] VALSKY, G.V., PETROV, G.A. and PLEVA, Yu.S., *Jadernaja Fizika* 8 (1968) 297.

[2] STANLEY Z., and WHETSTONE, F., *Phys. Rev.* 131 3 (1963) 1232.

	$E_K$	$J(90^\circ)$	$\Delta J(90^\circ)$	A	$\Delta A$
1.	155,0	1,407	0,321	- 0,019	0,204
2.	163,1	1,167	0,110	0,094	0,101
3.	171,3	1,138	0,078	0,095	0,055
4.	179,4	1,046	0,035	0,102	0,038
5.	187,5	1,000	0,028	0,138	0,034
6.	195,6	0,964	0,027	0,133	0,034
7.	203,8	0,913	0,031	0,135	0,043
8.	211,9	0,789	0,044	0,219	0,077
9.	220,0	0,640	0,072	0,460	0,187

V.G. Khlopin Radium Institute<sup>x/</sup>  
Leningrad

FRAGMENT SHELL-STRUCTURE  
EFFECTS IN NUCLEAR FISSION

V.A. Rubchenya  
(Submitted Jadernaja Fizika)

Using the Fong statistical fission model [1], the authors discuss the effect of the shell structure of nuclear fission fragments on the configuration of the fissioning system at the moment the neck breaks. The effect of the shell structure of the fragments is taken into account by using Strutinsky's method [2] to work out shell corrections to the nuclear-fragment masses. The calculations showed that at the moment the neck breaks the near-magic fragments are almost spherical (quadrupole deformation parameter  $\alpha \approx 0.05$ ) since the shell correction to the mass of these fragments, as calculated by a Weizsäcker-type semi-empirical mass formula, has a strongly negative value in the spherical state. The far-from-magic fragments are greatly stretched at the moment of rupture,  $\alpha \approx 0.50$ , because with these nuclei the shell correction for deformations  $\alpha \approx 2A^{1/3}$  has a strongly positive value.

Calculations for thermal fission of  $^{235}\text{U}$  and spontaneous fission of  $^{252}\text{Cf}$  give values of about 25 MeV and 10 MeV, respectively, for the dip in the curve of mean kinetic energy of fragments as a function of mass ratio in the symmetrical fission region, and this is in satisfactory agreement with experiment. The deformation energy of near-magic fragments is very low since at the moment the neck breaks they are almost spherical, while the deformation energy of complementary fragments is high because at the moment of splitting they are stretched so that the dependence of the calculated deformation energy on fragment mass reflects the serrated form of the experimental dependence of the average number of neutrons on the mass of the fragments.

---

<sup>x/</sup> Editor A.I. Obukhov.

THE DECAY OF AMERICIUM-242

B.M. Alexandrov, M.A. Bak, V.V. Berdikov, R.B. Ivanov,  
A.S. Krivokhatsky, V.G. Nedovesov, K.A. Petrzhak,  
Yu.G. Petrov, Yu.F. Romanov and Z.A. Shlyamin

(Submitted to Atomnaja energija)

The authors measured the half-life of americium-242 for the ground state using different methods, calculated the beta-decay/electron capture probability ratio and estimated the decay probability for this state. A sample containing americium-242 was obtained by neutron irradiation of americium-241 in the vertical channel of the VVR-M reactor with a flux density of approximately  $5 \times 10^{13}$  neutrons/cm<sup>2</sup> sec during a period of time comparable to the half-life of the isotope.

There are a large variety of methods of determining its half-life, due to the special nuclear physics properties of americium-242 and of its daughter products. The large fission cross-section under the effect of slow neutrons made it possible to observe how the number of fissions taking place in a thin target containing americium-242 changed with time when irradiated with a collimated beam of reactor-spectrum neutrons. These measurements were carried out in a double ionizing chamber using a uranium-235 target as flux monitor.

It was also possible to find the half-life by recording the increase in the alpha activity of the target, caused by the accumulation of curium-242 following the  $\beta$ -decay of americium-242. In this case the alpha-particle detector was a gold-silicon surface-barrier counter.

Since the alpha-decay energies of americium-241 and curium-242 differ considerably, the half-life could also be determined from the increase in the peak from  $\alpha$ -particles of curium-242. These measurements were carried out on an alpha spectrometer with a surface barrier counter.

The half-life of americium-242 was also determined by measuring the decrease in  $\beta$ -activity and the number of electron captures. Measuring the beta activity using a 4- $\pi$  methane flow counter required thorough cleaning of the americium-241 irradiated in the reactor and removal of all traces of fragments and accumulated plutonium and curium. Electron captures were recorded from plutonium-242 K radiation (approximately 100 keV) using a scintillation spectrometer with NaI(Tl) crystal.

The results are given in the table.

TABLE

Half-life of americium-242, as determined by different methods

Methods	Half-life (in hours)	Mean square error (in hours)
Americium-242 fission slow neutrons	16.1	0.2
Accumulation of curium-242	16.0	0.4
Increase in $\alpha$ peak from curium-242	16.0	0.4
$\beta$ -decay of americium-242	16.0	0.4
Electron capture	16.2	0.5

The half-life was found equal to  $16.07 \pm 0.04$  hours. This value was the weighted mean from the data in the table, and the error was calculated as the mean square of the weighted mean.

The beta-decay/electron capture probability ratio was determined by comparing the increase in  $\alpha$  activity of curium-242 with the decrease in X-radiation of energy approximately 100 keV which accompanies electron capture. These measurements were carried out, respectively, on an alpha spectrometer with a surface-barrier silicon detector and on a scintillation spectrometer with NaI(Tl) crystal. The probability ratio between electron capture and total decay of americium-242 from the ground state was found to be  $18 \pm 1\%$ . This gives a beta-decay/electron capture probability ratio of  $4.6 \pm 0.4$ .

The probability of  $\alpha$ -decay of americium-242 from the ground state was estimated using a magnetic alpha spectrometer. It was shown that if there is any  $\alpha$ -decay of americium-242 with an  $\alpha$ -particle energy in the range 5000-5300 keV, its probability is no more than  $10^{-7}$  of the total number of decays of americium-242 nuclei in the ground state.

[1] FONG, P., Phys. Rev. 102 (1956) 434.

[2] STRUTINSKY, V.M., Nucl. Phys. A95 (1967) 420.

TERNARY FISSION OF  $^{235}\text{U}$  BY SLOW NEUTRONS

V.M. Adamov, L.B. Drapchinsky, S.S. Kovalenko,  
K.A. Petrzhak and I.I. Tyutyugin

(Submitted to *Jadernaja Fisika*)

Surface-barrier detectors were used for simultaneously measuring the kinetic energy of fragments and of long-range alpha-particles in uranium-235 fission by slow neutrons. The work was carried out on the reactor at the A.F. Ioffe Institute of Physics and Technology. The mean total kinetic energy of ternary fission fragments was found to be 15 MeV less than in the case of binary fission. This figure is in good agreement with previous results. The total energy distribution half-width for ternary fission fragments is 4.7 MeV less than for binary fission fragments. The authors obtained a relation connecting the mean kinetic energy of the fragments and their dispersion kinetic energy with alpha-particle energy. The mean kinetic energy decreases linearly as the alpha-particle energy increases, with a slope  $\frac{\Delta E_k}{\Delta E_\alpha} = 0.35$ . Within the limits of experimental error the energy spread is independent of the alpha-particle energy. The mean alpha-particle energy decreases linearly as the total kinetic energy of the fragments increases, from 14.5 MeV at  $E_k = 140$  MeV, to 16 MeV at  $E_k = 170$  MeV. A relation was also found connecting the kinetic energy of light and heavy fragment groups with alpha-particle energy. From these data it can be assumed that the alpha-particle is formed essentially from nucleons of a heavy fragment.

Institute of Physics, Ukrainian SSR Academy of Sciences, Kiev<sup>\*/</sup>

NEUTRON CROSS-SECTIONS OF  $^{142}\text{Ce}$ ,  $^{140}\text{Ce}$ , NATURAL Ce AND  
 $^{164}\text{Dy}$  ABOVE 1 eV

V.P. Vertebny, P.N. Vorona, A.I. Kalchenko,  
M.V. Pasechnik, T.I. Pisanko, V.A. Pshenichny,  
and V.K. Rudyshin

The VVR-M reactor of the Institute of Physics, Academy of Sciences of the Ukrainian SSR, was used for transmission measurements on highly-enriched samples of  $^{142}\text{Ce}$  (93.4%),  $^{140}\text{Ce}$  (99.5%),  $^{164}\text{Dy}$  (97%) and natural cerium.

The number of nuclei per  $\text{cm}^2$  was:  $^{142}\text{Ce}$  -  $3.74 \times 10^{21}$ ;  $^{140}\text{Ce}$  -  $4.55 \times 10^{21}$ ; natural Ce -  $3.28 \times 10^{21}$ ;  $^{164}\text{Dy}$  -  $2.64 \times 10^{21}$  and  $5.29 \times 10^{21}$ . The resolution in the case of the cerium isotopes was  $0.55 \mu\text{sec/m}$ . For  $^{142}\text{Ce}$ , resonances were observed with energies  $1290 \pm 80$  eV and  $4380 \pm 500$  eV. There is every justification for assuming that  $^{142}\text{Ce}$  also has energy levels  $1640 \pm 240$  eV and  $2740 \pm 250$  eV. The level spacing observed for  $^{142}\text{Ce}$  was approximately 1000 eV, taking into account all these levels. For the 1290 eV level the authors obtained  $\Gamma_n = 47 \pm 2$  eV from measurements with a thin sample. With  $^{140}\text{Ce}$  no resonances were observed in the energy range 1-15 000 eV. For  $^{164}\text{Dy}$  measurements were carried out with resolutions 0.11 and 0.22  $\mu\text{sec/m}$ . There is a level  $146 \pm 6$  eV with a neutron width  $730 \pm 20$  meV. The data were processed by the area method. The radiation width was taken equal to 120 meV. The effect of the negative level can be observed up to 10-20 eV. The table gives total neutron cross-sections of  $^{164}\text{Dy}$  above 1 eV. The energy ranges in which there is an important contribution from other dysprosium isotopes are not included.

---

<sup>\*/</sup> Editor I.A. Korzha.

Table I

Neutron cross-sections  $^{164}\text{Dy}$ 

Energy (eV)	Cross-section in barns						
$E_v$	$\sigma_t$	$E_v$	$\sigma_t$	$E_v$	$\sigma_t$	$E_v$	$\sigma_t$
1.00	331 $\pm$ 6	2.82	113 $\pm$ 3	10.4	45	126	28
1.07	313	2.96	114	11.6	39	131	36
1.14	286	3.13	99	12.9	40	136	52 <sup>n</sup>
1.22	280	3.31	100	18.7	40 $\pm$ 2	141	142 <sup>n</sup>
1.31	263	3.53	99	21.7	35 $\pm$ 2	146	237 <sup>n</sup>
1.41	249 $\pm$ 5	4.29	88	25.3	33	152	139 <sup>n</sup>
1.99	167	4.54	76	29.9	31	158	72 <sup>n</sup>
2.08	164 $\pm$ 5	4.88	79	35.9	29	164	45 <sup>n</sup>
2.19	152	6.61	52	43.8	26 $\pm$ 2	172	39
2.29	151	7.13	53 $\pm$ 2	70.2	24	195	26
2.40	137	7.78	49	94	24	247	28
2553	131	8.53	40	100	21	322	30 $\pm$ 2
2.66	135	9.43	38	114	25		

<sup>n</sup>Cross-sections averaged for distribution function.

ENERGY DEPENDENCE OF THE TOTAL NEUTRON CROSS-SECTION OF OSMIUM-187  
IN THE ENERGY RANGE 0.006-0.3 eV

V.P. Vertebny, M.F. Vlasov, A.F. Dedakina,  
R.A. Zatserkovsky, A.L. Kirilyuk, N.V. Pasechnik  
and N.A. Trofimova

The VVR-M reactor of the Institute of Physics, Academy of Sciences of the Ukrainian SSR, with a resolution of 7  $\mu$ sec/m was used to measure the total neutron cross-section of the isotopes osmium-187, osmium-188, osmium-189 and natural osmium, in the energy range 0.006-0.3 eV. The measurements were made with samples in the form of metallic powders. The "osmium-187" sample was enriched to 31.5% in the isotope being studied. The results are given in the table. The contribution of positive levels to the 2200 m/sec cross-section for osmium-187 is about 6 barns.

Since the scattering cross-section for osmium-187 is of the order of 8-15 barns the remaining 320 barns can be explained only by a contribution of negative levels. The total cross-section in the energy range 0.008-0.04 eV is described to an accuracy of more than 5% by the formula:

$$\sigma_t = 7.4 + \frac{53.1}{\sqrt{E}}$$

The energy dependence of the total neutron cross-section of osmium-187 (E = energy in eV,  $\sigma_t$  = cross-section in barns) is given in the table.

Table

$E$ (v)	$\sigma_t$ (barn)	$E$ (eV)	$\sigma_t$ (barn)	$E$ (eV)	$\sigma_t$ (barn)
0,279	119 $\pm$ 9	0.0290	317	0.0103	519
0,253	103	0,0281	329	0.0101	570
0.230	121	0.0272	322	0.00994	558
0.211	130	0.0264	314	0,00976	570
0.194	134	0.0256	343	0.00957	574
0.179	130	0.0249	343 $\pm$ 12	0,00939	539
0.165	148	0.0241	358	0.00922	560
0.153	145	0.0234	356	0.00906	602
0.142	146	0.0228	357	0.00890	563
0.133	158	0.0221	376	0.00875	603
0.124	167	0.0215	373	0.00859	607
0.116	170	0.0209	360	0.00844	585
0.109	174	0.0204	387	0.00830	606
0.103	178	0.0198	388	0.00816	600
0.0965	188	0.0193	391	0.00802	597
0.0911	187	0.0188	398	0.00788	634
0.0861	200	0.0183	406	0.00775	646 $\pm$ 40
0.0815	199	0.0179	408	0.00762	583
0.0773	220	0,0174	404 $\pm$ 13	0.00750	611
0.0734	227	0.0170	424	0.00738	588
0.0698	215 $\pm$ 10	0.0166	416	0.00726	606
0.0664	217	0.0162	436	0.00714	566
0.0633	226	0.0158	448	0.00703	644
0.0604	226	0.0154	431	0.00692	589
0.0576	237	0.0151	435	0.00681	674
0.0551	247	0.0147	427	0.00671	600
0.0527	247	0.0144	464	0.00660	679
0.0505	235	0.0141	449	0.00650	766
0.0484	251	0.0138	446	0.00641	641
0.0465	261	0.0135	469	0.00631	607
0.0446	265	0.0132	490	0.00622	608
0.0429	261	0.0129	473	0.00613	603
0.0413	274	0.0126	483	0.00604	703
0.0397	280	0.0124	510	0.00595	944
0.0383	287	0.0121	506	0.00586	742
0.0369	282	0.0119	502	0.00578	754 $\pm$ 100
0.0356	307	0.0116	494		
0.0343	277	0.0114	543		
0.0332	309	0.0112	518 $\pm$ 19		
0.0320	312	0.0109	526		
0.0310	316 $\pm$ 11	0.0107	523		
0.0300	318	0.0105	529		

TOTAL SCATTERING CROSS-SECTIONS OF SLOW NEUTRONS ON NATURAL YTTERBIUM

V.P. Vertebny, N.L. Gnidak, E.A. Pavlenko  
and M.V. Pasechnik

The total scattering cross-section of natural ytterbium was measured on the VVR-M reactor of the Institute of Physics, Academy of Sciences of the Ukrainian SSR, with  $4\pi$  geometry and a resolution of 6-12  $\mu\text{sec}/\text{m}$ , in the neutron energy range 0.025-4 eV.

The measurements were carried out relative to vanadium. The cross-section for vanadium was taken equal to 4.15 barns. The samples of ytterbium were in the form of the oxide  $\text{Yb}_2\text{O}_3$ . The thickness of the sample was  $7.57 \times 10^{20}$  nuclei/cm<sup>2</sup>. Impurities had no marked effect. The samples were heated at 700°C for three hours. A correction of 8-14% was made for self-screening and neutron absorption. The oxygen cross-section was taken equal to 3.8 barns. It was assumed that the energy dependence of magnetic scattering on  $\text{Yb}^{+++}$  has the same form as for  $\text{Er}^{+++}$ , namely

$$\sigma_{\text{Yb}^{+++}}/\sigma_{\text{Er}^{+++}} = 0.224$$

corresponding to the value of the magnetic moments. The data, averaged for different resolutions, are given in the table. The magnetic scattering cross-sections were subtracted.

$E$ , eV	$\sigma_s$ , barn	$E$ , eV	$\sigma_s$ , barn
4.06	18.6	0.134	25.0
2.98	19.1	0.126	25.1
2.28	20.5	0.119	25.2 ± 0.4
1.80	21.6	0.114	25.0
1.46	22.5 ± 0.5	0.107	25.0
1.21	23.8	0.101	25.0
1.014	24.0	0.096	25.2
0.86	24.6	0.0913	25.3 ± 0.3
0.745	24.5	0.087	25.3
0.65	26.3 ± 0.5	0.083	25.3
0.57	26.8	0.079	25.3
0.505	26.2	0.075	25.2
0.45	24.7	0.072	25.1 ± 0.3
0.404	23.8	0.069	24.9
0.365	24.0 ± 0.5	0.066	25.0
0.33	23.8	0.063	35.0
0.30	23.9	0.061	25.2
0.28	24.0	0.058	24.5 ± 0.3
0.25	24.9	0.056	24.1
0.234	25.3 ± 0.5	0.054	24.0
0.216	25.6	0.052	24.5
0.2	25.4	0.050	25.0
0.186	25.3	0.048	25.2 ± 0.4
0.174	25.2	0.0466	24.8
0.16	25.2 ± 0.4	0.045	24.5
0.152	25.1	0.04	24.1 ± 0.4
0.143	25.0	0.025	24.6 ± 0.9

DETERMINING THE OPTICAL SCATTERING LENGTHS R' OF EVEN-EVEN NUCLEI  
FROM NEUTRON SCATTERING CROSS-SECTION MEASUREMENTS

V.P. Vertebny, N.L. Gnidak, V.V. Koloty and E.A. Pavlenko

The expression

$$R' = a + \frac{1}{2} \sum \frac{\lambda_r \Gamma_n^{(r)}}{E_r},$$

(where  $a$  is the scattering amplitude and  $\Gamma_n^{(r)}$ ,  $E_r$  and  $\lambda_r$ , respectively, are the neutron width, resonance energy and derived neutron wave length in the resonance) was used to determine the optical scattering lengths  $R'$  from measured scattering cross-sections of thermal and epithermal neutrons on isotopes. For positive levels the resonance parameters were taken from the measurements. The negative level parameters were estimated from the capture cross-sections using the Porter-Thomas and Wigner distributions.

In all cases, the second term on the right-hand side was small compared with  $a$ . The values obtained for  $R'$  are given in the table.

Isotope	<i>Er 140</i>	<i>Er 168</i>	<i>Er 166</i>	<i>Dy 164</i>	<i>Cd 116</i>	<i>Cd 114</i>	<i>Cd 112</i>
R' in fermis	$10.3 \pm 1$	$10.5 \pm 0.6$	$9.6 \pm \frac{2}{1}$	$8.7 \pm 1$	$7.2 \pm \frac{0.4}{1,6}$	$\leq 6.5$	$7.4 \pm \frac{0.3}{-0.7}$

ABSOLUTE MEASUREMENTS, BY MEANS OF A NEUTRON SELECTOR, OF INTEGRAL  
DOSES OF SLOW NEUTRONS IN THE ACTIVE ZONE OF A NUCLEAR REACTOR

V.P. Vertebny, R.A. Zatserkovsky and A.L. Kirilyuk

The authors describe an absolute method of measuring integral doses of slow neutrons above  $10^{17}$  neutrons/cm<sup>2</sup>. The method is based on transmission (T) measurements on spent absorbers before and after irradiation in the active zone of a reactor.

Various methods, involving the use of a neutron selector, neutron filters and a "white" neutron spectrum from a reactor channel are considered. The possibility of measuring neutron gas temperatures is discussed.

Institute of Nuclear Power Engineering,  
BSSR Academy of Sciences, Minsk\*/  
Byelorussian SSR

AN ANALYTICAL MODEL FOR EFFECTIVE CROSS-SECTIONS OF NUCLEAR REACTIONS  
ON THERMAL NEUTRONS

V.A. Naumov and A.P. Semashko

The authors propose the following analytical model (1)

$$\langle \sigma_z^\alpha \rangle_T = \int_0^{E_T} \tilde{\sigma}_z^\alpha(E) \Phi(E, T) dE / \int_0^{E_T} \Phi(E, T) dE,$$

where  $\alpha$  is the isotope index,  $\lambda$  is the type of nuclear reaction (absorption, fission, etc.) to describe the dependence of the effective cross-sections of thermal neutron nuclear reactions for nuclei having the isotopic composition of a homogeneous (homogenized) reactor medium

$$\langle \sigma_z^\alpha \rangle_T = \langle \sigma_z^\alpha \rangle_M \frac{1 + C(T) \frac{\langle \Sigma_a \rangle_M}{\bar{\xi} \Sigma_s} \langle \sigma_z^\alpha \rangle_S / \langle \sigma_z^\alpha \rangle_M}{1 + C(T) \frac{\langle \Sigma_a \rangle_M}{\bar{\xi} \Sigma_s}}$$

on poisoning, temperature and nuclear chemical bond.

The proposed analytical model describes the dependence of the effective nuclear cross-sections on poisoning, temperature and chemical bond, in the range of variation of practical interest, with an accuracy of 1%. The results of a comparison of effective cross-sections calculated from this model in conjunction with a rigorous solution of the kinetic equation [1], are given in Tables I-III,

---

\*/ Editor V.A. Naumov

[1] DUNETS, E.M., NAUMOV, V.A., SEMASHKO, A.P., Proceedings of the Conference on Reactor Physics, Vol. 2 Melekess 1966.

TABLE I

Comparison of effective absorption cross-sections ( $1/v$  law) for thermal neutrons in water, as calculated from the "PRES" programme (A) and from formula (1)(B) for different temperature and poisoning conditions

$\sigma_a^b$	Effective cross-section $\langle 1/v \rangle_T$						Model (1) parameters		
	0,01	0,1	1	2	3	10	$C(T)$	$\langle 1/v \rangle_M$	$\langle 1/v \rangle_S$
$T, K$	-	-	-	-	-	-	$C$		
A	0,87293	0,86958	0,83833	0,80783	0,78099	0,656214			
B	0,87581	0,87276	0,83948	0,80690	0,77819	0,644266	1,5	0,8762	0,320
$\frac{B-A}{A} \%$	+ 0,32	+ 0,18	+ 0,18	+ 0,0013	- 0,16	- 1,36			
A	0,61898	0,61794	0,60794	0,59765	0,58813	0,537272			
B	-	0,61872	0,60603	0,59315	0,58138	0,520780	1,5	0,6202	0,320
$\frac{B-A}{A} \%$	-	+ 0,12	- 0,31	- 0,75	- 1,15	- 3,08			
A	0,50909	0,50862	0,50411	0,49937	0,49488	0,469310			
B	0,51002	0,50933	0,50266	0,59578	-	0,455086	1,5	0,5101	0,320
$\frac{B-A}{A} \%$	+ 0,18	+ 0,14	- 0,29	- 0,72	-	- 3,03			
A	0,44944	0,44919	0,44679	0,44424	0,44179	0,427319			
B	0,44995	0,44954	0,44551	0,44129	0,43735	0,415730	1,5	0,4500	0,320
$\frac{B-A}{A} \%$	+ 0,11	+ 0,08	- 0,29	- 0,66	- 1,00	- 2,71			

TABLE II

Comparison of effective absorption cross-section ( $1/v$  law) for thermal neutrons in zirconium hydride, as calculated from the "PRES" programme (A) and from formula (1)(B) for different temperature and poisoning conditions

	$\zeta_a^0$	Effective cross-section $\langle 1/v \rangle_T$						Model (1) parameters		
		0,01	0,1	1	2	3	10	$C(T)$	$\langle 1/v \rangle_H$	$\langle 1/v \rangle_L$
$T^{\circ}K$	-	-	-	-	-	-	-			
A	0,86801	0,85616	0,77271	0,71853	0,68219	0,567320				
B	0,87602	0,87490	0,78000	0,71160	0,66177	-	4,4	0,8762	0,320	
$\frac{B-A}{A} \%$	+ 0,92	+ 1,19	+ 0,91	- 0,96	- 3,0	-				
A	0,75402	0,74904	0,708262	0,67554	0,65052	0,556609				
B	-	-	0,710523	0,67169	0,640082	0,515869	3,0	0,7590	0,320	
$\frac{B-A}{A} \%$	-	-	+ 0,30	- 0,59	- 1,50	- 7,20				
A	0,67561	0,67307	0,65049	0,63055	0,61303	0,539540				
B	0,67856	0,67642	0,65639	0,63726	0,61905	0,535362	1,8	0,6788	0,320	
$\frac{B-A}{A} \%$	+ 0,40	+ 0,49	+ 0,91	+ 0,79	+ 1,08	- 0,76				
A	0,61767	0,61615	0,60211	0,58855	0,57665	0,519840				
B	0,62005	0,61868	0,60571	0,59256	0,58056	0,519188	1,5	0,6202	0,320	
$\frac{B-A}{A} \%$	+ 0,31	+ 0,42	+ 0,67	+ 0,68	+ 0,69	- 0,15				

TABLE III

Comparison of effective cross-sections for thermal neutron absorption by the isotopes  $^{235}\text{U}$  and  $^{239}\text{Pu}$  in water, as calculated from the "PRES" programme (A) and from formula (1)(B) for different temperature and poisoning conditions.

		Effective cross-section $\langle \sigma_a^{U-235} \rangle_T$						Model (1) parameters			
		$\sigma_a^0$	0,01	0,1	1	2	3	10	$C(T)$	$\langle \sigma_a \rangle_M$	$\langle \sigma_a \rangle_S$
$T^{\circ}\text{K}$											
A	300	581,779	579,360	556,832	534,888	515,614	426,580				
B		586,330	583,913	561,323	539,144	519,540	427,473	1,5	586,6	200	
$\frac{B-A}{A} \%$		0,78	0,79	0,80	0,80	0,76	0,21				
A	600	394,690	393,991	387,288	380,401	374,038	340,160				
B		397,900	397,025	388,659	380,158	372,393	332,429	1,5	398,0	200	
$\frac{B-A}{A} \%$		0,82	0,77	0,35	- 0,64	- 0,44	- 2,27				
A		283,240	283,079	281,502	279,825	278,222	268,720				
B	1200	284,070	283,799	281,182	278,462	275,915	261,872	1,4	284,1	200	
$\frac{B-A}{A} \%$		+ 0,29	+ 0,025	- 0,011	- 0,49	- 0,83	- 2,54				

		Effective cross-section $\langle \sigma_a^{Pu-239} \rangle_T$						Model (1) parameters			
		$\sigma_a^0$	0,01	0,1	1	2	3	10	$C(T)$	$\langle \sigma_a \rangle_M$	$\langle \sigma_a \rangle_S$
$T^{\circ}\text{K}$											
A		970,297	973,172	1001,14	1029,79	1056,23	1199,31				
B	300	970,480	973,880	1014,91	1054,29	1089,21	1052,65	1,5	9,700	1656	
$\frac{B-A}{A} \%$		+ 0,024	+ 0,073	+ 1,38	+ 2,38	+ 3,12	+ 4,45				

Joint Institute for Nuclear Research<sup>\*/</sup>

NEUTRON RESONANCES OF THE ISOTOPE<sup>s</sup>  $^{69}\text{Ga}$  AND  $^{71}\text{Ga}$

Kh. Maletski, L.B. Pikelner, I.M. Salamatin and E.I. Sharapov

Measurements of transmission, self-induction and radiative capture of neutrons were carried out for  $^{69}\text{Ga}$  and  $^{71}\text{Ga}$  nuclei using the time-of-flight method on the IBR pulsed reactor with a microtron. The flight-path length was 1000 m (for transmission measurements) and 242 m (for self-induction and radiative capture measurements) with a neutron pulse half-width of 3  $\mu\text{sec}$ .

Measurements were carried out with samples of two or three thicknesses and in the radiative capture measurements enriched isotopes were used.

The measurement data were processed on a computer and values of  $g\Gamma_n$  (Table 1) were obtained by the area method. The spins  $J$  and total radiation widths  $\Gamma_\gamma$  were found for 18 levels with  $\Gamma_n \gg \Gamma_\gamma$  using a method similar to that in ref. [1].

Table 2 gives the force functions  $S_0(J)$  for two spin states, mean values (for two values of  $J$ ) of  $S_0$ , mean spacing between  $s$ -resonances, mean total radiation widths and values of the parameter  $a$  for the density of single particle states close to the Fermi surface.

The values of  $S_0(J)$  obtained do not indicate that there is a difference in the force functions for the two spin systems of  $^{69}\text{Ga}$ , as claimed in reference [2] on the basis of less exhaustive experimental data.

---

<sup>\*/</sup> Editor Yu. P. Popov

REFERENCES

- [1] MALETSKI, Kh., PIKELNER, L.B., SALAMATIN, I.M., SHARAPOV, E.I.,  
Joint Institute of Nuclear Research, Preprint RZ-3956, Dubna, 1968.
- [2] JULIEN, J., BIANCHI, G., CORGE, C., et al., Phys. Lett. 10 (1964) 86.

Table 1

Neutron resonance parameters of gallium isotopes

Target nucleus	$E_0$ eV	$\Delta E$ eV	$\gamma$ eV	$g\Gamma_m$ eV	$\Delta g\Gamma_m$ eV	$\Gamma_\gamma$ eV	$\Delta\Gamma_\gamma$ eV
I	2	3	4	5	6	7	8
Ga -69	III	0,5	2	0,034	0,003	0,270	0,06
	334	0,7		0,12	0,025		
	473	I	I	0,072	0,010	0,260	0,060
	532 <sup>x</sup>	2		0,0021	0,0004		
	611 <sup>x</sup>	2		0,0026	0,0004		
	692	2	2	0,77	0,11	0,270	0,040
	941 <sup>x</sup>	3		0,0026	0,0005		
	1252 <sup>x</sup>	5		0,0035	0,0010		
	1354	5	2	0,17	0,03	0,290	0,060
	1579	6	2	1,20	0,24	0,260	0,040
	1636	7	I	1,8	0,16	0,260	0,040
	1866	9	2	1,5	0,24	0,250	0,040
	1906 <sup>x</sup>	9		0,006	0,003		
	1994 <sup>x</sup>	10		0,006	0,003		
	2167 <sup>x</sup>	11		0,0075	0,0022		
	2452	13	I	4,5	0,5	0,290	0,040
	2989 <sup>x</sup>	19		0,04	0,02		
	3084	20		0,11	0,04		
	3377 <sup>x</sup>	22		0,01	0,005		
	3497	22	2	11,2	1,0	0,260	0,041
	3739 <sup>x</sup>	26		0,012	0,005		
	3873	28		0,020	0,006		
	3970	30		0,01	0,007		
	4206	30		0,83	0,30		
	4361	32		0,94	0,40		
	4556	35		0,2	0,1		
	4810	37		9			
	5280	42					
	5666	46					
	5877	50					

Ga -7I	95,8	0,4	2	0,062	0,012	0,260	0,060
	287,5	1,7	2	3,9	0,5	0,240	0,040
	376	0,8	1	1,37	0,11	0,240	0,030
	705	2	2	0,28	0,04	0,230	0,035
	1092 <sup>x</sup>	4		0,0050	0,0014		
	1135 <sup>x</sup>	9		0,074	0,0022		
	1481 <sup>x</sup>	13		0,007	0,004		
	1525	7	2	2,04	0,25	0,220	0,035
	1870 <sup>x</sup>	9		0,008	0,004		
	1930	10	1	0,28	0,08	0,220	0,040
	2400	12	1	2,1	0,4	0,250	0,040
	2784	16	2	0,76	0,14	0,230	0,035
	2880 <sup>x</sup>	18		0,04	0,02		
	3110 <sup>x</sup>	10		0,03	0,02		
	3200 <sup>x</sup>	20		0,06	0,03		
	3311	20	1	2,0	0,4	0,240	0,035
	3400 <sup>x</sup>	23		0,06	0,03		
	3510 <sup>x</sup>	24		0,02	0,01		
	3790 <sup>x</sup>	28		0,02	0,01		
	4170	30		0,09	0,06		
	4690	36		0,6	0,30		
	4810	38		9			
	5054	40		6,1	1,3		

<sup>x</sup> Proposed p-wave resonances

Table 2

Mean parameters for gallium isotopes

Isotope Ga	$S_{0, \gamma=1}$	$S_{0, \gamma=2}$	$S_0$	$\bar{D}$ obs eV	$a$ MeV <sup>-1</sup>	$\bar{\Gamma}_r$ eV
69	1,0 $\begin{smallmatrix} +2 \\ -0,4 \end{smallmatrix}$	1,1 $\begin{smallmatrix} +1 \\ -0,4 \end{smallmatrix}$	1,1 $\begin{smallmatrix} +0,9 \\ -0,3 \end{smallmatrix}$	230 ± 55	11,2 ± 0,3	0,27 ± 0,94
71	1,3 $\begin{smallmatrix} +2,5 \\ -0,5 \end{smallmatrix}$	1,5 $\begin{smallmatrix} +2 \\ -0,5 \end{smallmatrix}$	1,4 $\begin{smallmatrix} +1,3 \\ -0,5 \end{smallmatrix}$	330 ± 70	12,3 ± 0,3	0,24 ± 0,04

(n,α) REACTIONS ON RESONANCE NEUTRONS CLOSE TO SHELLS WITH  
N = 50 AND Z = 50

Yu.P. Popov, M. Florek

The time-of-flight method was used on the IBR pulsed reactor with a microtron as injector to investigate (n,α) reactions on natural mixtures of isotopes of palladium and xenon and on enriched isotopes of molybdenum-95 and tellurium-123.

α-widths were measured and spins determined for three <sup>95</sup>Mo resonances and three <sup>123</sup>Te resonances. The estimated maximum α widths are given for several <sup>105</sup>Pd and <sup>129</sup>Xe resonances (see table).

The authors introduce the concept of an α-particle force function and discuss possible reasons for the excessive values of the α-particle force function calculated from the statistical theory, as compared with the experimental data.

Table

Target nucleus	E <sub>0</sub> eV	J	Other authors J	Γ <sub>α</sub> MeV	Γ <sub>α</sub> <sup>stat</sup> MeV
<sup>95</sup> Mo	45,1	3	3	≤ 0,018	15
	158,5		3	≤ 4,0	"
	358,2		3	≤ 1,6	"
	553,9	2	2	6,3 ± 3,6	290
	899	2	2	1,6 ± 12	"
	1145	2	2	39 ± 25	"
<sup>123</sup> Te	2,33	1	1	≤ 0,004	0,007
	24,1		0	≤ 0,1	4,0
	35,9			≤ 0,35	"
	96,9	0		3,3 ± 1,9	4,0
	235,3	0		5,3 ± 3,8	"
	275	0		3,4 ± 2,9	"
<sup>105</sup> Pd	13,2		2	≤ 0,06	0,82
	30,2		2	≤ 3,4	"
	78,5		2	≤ 0,6	"
<sup>129</sup> Xe	9,4	(1)	1	≤ 0,004	0,004
	92,2		1	≤ 0,02	"
	125,8		0	≤ 0,03	0,25

RADIATIVE CAPTURE AND TOTAL CROSS-SECTIONS FOR NEUTRON  
INTERACTION WITH SELENIUM ISOTOPES

Kh. Maletsky, L.B. Pikelner,  
I.M. Salamatin, E.I. Sharapov

Neutron transmission and radiative capture measurements were performed for separated selenium isotopes using the IBR pulsed reactor with a microtron and resolutions of 6 and 12 nsec/m, respectively.

Level parameters were obtained for  $^{74}\text{Se}$  and  $^{76}\text{Se}$  in the energy interval up to 10 keV, for  $^{78}\text{Se}$  and  $^{80}\text{Se}$  up to 20 keV and for  $^{77}\text{Se}$  up to 4 keV (see Table 1). The spins of 15 levels with  $\Gamma_n > \Gamma_\gamma$  were obtained for the odd isotope in the energy range studied. The level parameters found were used for calculating various mean nuclear parameters (see Table 2). The force functions  $S_0$  of the isotopes studied are in agreement with the data for neighbouring nuclei. In the case of  $^{77}\text{Se}$  no spin dependence was observed for  $S_0$  and  $\Gamma_\gamma$  in the energy range up to 4 keV.

Table I

Neutron resonance parameters of selenium isotopes

Target nucleus	$E_0$ eV	$\Delta E_0$ eV	$\gamma$	$g\Gamma_n$ eV	$\Delta g\Gamma_n$ eV	$\Gamma_\gamma$ eV	$\Delta\Gamma_\gamma$ eV
Se -74	27,1	0,1		0,17	0,025	0,280	0,080
	271,5	1,0		4,75	0,18	0,300	0,045
	1029	3,6		2,37	0,38	0,300	0,045
	1386	6,0		1,22	0,09	0,320	0,048
	1630	7,0		0,14 <sup>±</sup>	0,04		
	1746	8,0		9,86	0,60	0,270	0,054
	2303	24,0		1,61	0,44	0,280	0,050
	7216	68,0		10,64	3,90		
Se -76	378	0,8		0,336	0,020	0,220	0,033
	864	2,8		3,31	0,24	0,220	0,033
	920	3,2		0,040 <sup>±</sup>	0,008		
	1210	4,6		0,027 <sup>*</sup>	0,005		
	1355	10		0,023 <sup>±</sup>	0,004		
	1480	12		0,016 <sup>±</sup>	0,004		
	1646	7,4		0,008 <sup>±</sup>	0,004		
	2120	13		0,107	0,015		
	2575	14		14,24	0,85	0,230	0,046
	3170	20		0,049 <sup>*</sup>	0,010		
	3363	21		14,0	0,9	0,250	0,050
	3940	27		0,220	0,050		
	4313	32		4,0	2,0	0,210	0,050
	5020	39		< 0,5 <sup>±</sup>			
	5387	48		38,5	8,4		
	64,37	57		18,0	2,0		
	7148	66		22,8	3,5		
	8480	129		2,7	1,3		
	10210	113		20,8	4,7		
	11320	200		2,3	1,5		
13281	251		25,2	9,1			

Se -77	II2			0,0013	0,0002		
	I5I,6	I,0		0,00019*	0,00006		
	I76,4	I,0		0,00037*	0,0001		
	2I2	0,8	0	0,380	0,02	0,380	0,060
	29I	0,8		0,0093	0,0009		
	34I,5	I,0		0,065	0,012		
	369	0,8		0,0012*	0,0006		
	443	I,0		0,0047*	0,0007		
	483	I,2		0,0083	0,0012		
	5I7	I,3		0,0025*	0,0005		
	552	I,4		0,0043*	0,0007		
	692	2,0	0	0,60	0,03	0,330	0,050
	864	2,8		0,46	0,08		
	970	3,3	(I)	0,095	0,030		
	997	3,5	0	2,20	0,40	0,450	0,080
	I090	4,0		0,075	0,025		
	I27I	8,0	I	0,86	0,08	0,460	0,080
	I300	5		0,0076*	0,003		
	I333	5		0,009*	0,003		
	I402	6		0,10	0,03		
	I466	6		0,014	0,005		
	I49I	6	0	0,240	0,035	0,350	0,100
	I530	7		0,0058*	0,001		
	I687	8	I	0,52	0,10	0,520	0,150
	I795	8		0,10	0,05		
	I860	9		0,024	0,007		
	I880	9		0,012*	0,004		
	2040	10		0,25	0,10		
	2267	I2	I	I,15	0,24	0,390	0,060
	232I	I2	I	3,5	I,0	0,350	0,050
	2540	28	I	2,5	0,5	0,340	0,050
	2664	23	I	0,86	0,22	0,390	0,060
	3034	27	I	0,60	0,20	0,600	0,250
	3I97	20	I	2,2	0,3	0,440	0,080
	3342	2I	0	I,20	0,25	0,360	0,050
	3554	23	I	I,85	0,30	0,360	0,060
	39I9	40	I	2,0	0,4	0,390	0,060

<i>Se-78</i>	384	0,8	0,33	0,03	0,180	0,030
	850	4	0,022*	0,004		
	1350	8	0,026*	0,005		
	2027	15	0,150*	0,030		
	2397	20	0,127*	0,025		
	3227	20	12,3	0,7	0,260	0,055
	3852	40	0,36	0,18		
	4626	35	0,39	0,17		
	5673	47	1,8	1,0	0,230	0,050
	6189	54	64,4	3,0		
	6857	63	3,5	1,8	0,220	0,050
	9250	98	39,0	6,0		
	11066	129	80,0	6,0		
	19100	292	23,0	8,0		
	<i>Se-80</i>	20150	316	17,0	5,0	
1740		10	0,050*	0,013		
1970		19	55	4		
4270		31	59	13		
4720		36	4,8	2,4	0,250	0,100
5100		40	74	19		
5240		43	< 0,6*			
5660		46	7	4	0,210	0,055
6120		52	< 0,7*			
8150		80	< 0,9*			
12632		156	26	8		
20300		320	123	23		
23122	390	48	15			

Asterisks indicate assumed p-wave resonances.

Table 2

Averaged parameters for selenium isotopes

Isotope	Se - 74	Se - 76	Se - 77	Se - 78	Se - 80	
Number of levels studied	8	21	37	15	12	
$S_0 \cdot 10^{-4}$	2,6 + 3,0 - 0,9	1,7 + 1,1 - 0,5 ( $J = 0$ )	1,4 + 1,6 - 0,5 ( $J = 1$ )	1,1 + 0,6 - 0,3	1,9 + 1,3 - 0,5	2,0 + 2,0 - 0,7
$\bar{\Gamma}_\gamma$ , MeV	290 ± 50	230 ± 40	390 ± 70	220 ± 45	220 ± 50	
$\bar{D}$ observed $d$ - levels, eV	370 ± 70	700 ± 150	120 ± 20	1000 ± 270	1200 ± 380	
$\alpha$ , MeV <sup>-1</sup>	14,1 ± 0,5	14,3 ± 0,4	14,1 ± 0,3	14,0 ± 0,5	14,7 ± 0,7	

DETERMINING THE NUCLEAR SCATTERING AMPLITUDES OF TUNGSTEN  
ISOTOPES BY THE NEUTRONOGRAPHIC METHOD

Yu.A. Alexandrov, A.M. Balagurov, E. Malishevsky,  
T.A. Machekhina, L.N. Sedlakova and Ya. Kholas

JINR preprint P3-4121, Dubna, 1968

The method of neutron diffraction on powders and single-crystals was used to measure the nuclear scattering amplitudes of the following tungsten isotopes:  $^{182}\text{W}$ ,  $^{183}\text{W}$ ,  $^{184}\text{W}$  and  $^{186}\text{W}$ . The following amplitudes were obtained, in units of  $10^{-12}$  cm:  $b_2 = 0.833 \pm 0.014$ ,  $b_3 = 0.43 \pm 0.05$ ,  $b_4 = 0.759 \pm 0.009$  and  $b_6 = -0.119 \pm 0.05$ .

Owing to the interference of potential and resonance scattering, the  $^{186}\text{W}$  amplitude was negative and anomalously small. This fact can be used to study effects which are concealed by strong nuclear scattering, in particular for precision measurements of neutron and electron interaction.

THE VARIATION IN KINETIC ENERGY OF FRAGMENTS IN  $^{235}\text{U}$  FISSION  
BY NEUTRONS OF ENERGY 0.006-20 eV

S. Bochvarov, E. Dermendzhiev and N. Kashukeev

JINR preprint P3-4110, Dubna, 1968

The LNF neutron spectrometer of the Joint Institute of Nuclear Research was used in studying the variation in the kinetic energy  $E_k$  of fragments in the thermal range and in 11  $^{235}\text{U}$  resonances: the method adopted was to measure the relative yield  $W$  of fragments from two targets of different thickness with neutrons in the energy range 0.006-20 eV. It was found that the resonances 0.29 eV, 2.04 eV, 3.14 eV, 4.84 eV, and 7.09 eV can be put into a group of resonances with smaller  $W$ , and hence smaller  $E_k$ , while the resonances 1.14 eV, 3.60 eV, 6.40 eV, 8.78 eV, 12.4 eV and 19.3 eV form a group with larger  $W$  and larger  $E_k$ . A comparison of the  $W$  values with radiochemical data on fission fragment yields in the thermal range and in  $^{235}\text{U}$  resonances shows that  $E_k$  is apparently larger in the case of more asymmetric fission. The variations in the mean total kinetic energy of the fragments,  $2\overline{\Delta E}_k = 0.74 \pm 0.32$  MeV, was determined from the values  $W(\text{I})$  and  $W(\text{II})$  for the two resonance groups.

A STUDY OF  $\gamma$ -RAY SPECTRA FROM THE REACTION  $^{127}\text{I} (n, \gamma) ^{128}\text{I}$   
FOR RESONANCE NEUTRONS

F. Bechvarzh, Ya. Gronik, E.Z. Ryndina, S.A. Telezhnikov,  
Ya. Urbanets and Yu. Shakha

(Presented at the XIXth Conference on Nuclear  
Spectroscopy, Yerevan, 1969)

Using the JINR pulsed fast reactor with time-of-flight methods and a Ge(Li) detector with a sensitive volume of  $30 \text{ cm}^3$ , the authors measured gamma-ray spectra from the reaction  $^{127}\text{I} (n, \gamma) ^{128}\text{I}$  in ten different resonances. A group of strong transitions with unresolved energies of about 6690 keV was found. This group fluctuates from one resonance to another in accordance with the Porter-Thomas law with  $\sim 4$ . The average intensity of the group is twice as high as the average intensity of the other four transitions.

There is considerable progressive interference in the yield cross-section for the group with energies about 6690 keV between the 31.2 and 37.7 eV resonances.

A marked difference was noted between the gamma-ray spectrum from the 20.4 eV resonance and the gamma-ray spectrum averaged over the remaining resonances.

Possible explanations are given for these findings.

#### NEW EXPERIMENTAL INSTALLATIONS

At the beginning of 1968 physics experiments were started in the Institute of Physics and Power Engineering using the EGP-10 electrostatic accelerator with ion recharging. This accelerator, which was developed by the Scientific Research Institute for Electrical and Physics Equipment in Leningrad, is intended for accelerating protons and neutrons to an energy of 10 MeV at a current of about 2  $\mu$ A. At present the accelerator is being used with semiconductor detectors to study the processes of elastic and inelastic scattering of protons on different nuclei at energies up to 8 MeV.

C O N T E N T S

I. Abstracts

- (1) Institute of Physics and Power Engineering
- (2) I.V. Kurchatov Atomic Energy Institute
- (3) Institute of Theoretical and Experimental Physics
- (4) A.F. Ioffe Physico-Technical Institute
- (5) V.G. Khlopin Radium Institute
- (6) Institute of Physics, Academy of Sciences, Ukrainian SSR
- (7) Institute of Nuclear Power Engineering, Academy of Sciences,  
Byelorussian SSR
- (8) Joint Institute of Nuclear Research.

II. Statement regarding new experimental installations.